ESCUELA SUPERIOR POLITÉCNICA DEL LITORAL

Facultad de Ingeniería en Ciencias de la Tierra

"DETERMINACIÓN DEL FACTOR DE SEGURIDAD PARA TALUDES ANISOTRÓPICOS EN LAS ÁREAS MINERAS "VICTORIA I" Y "VICTORIA II", UTILIZANDO LOS SISTEMAS DE EVALUACIÓN DE BIENIAWSKY Y ROMANA Y MÉTODO DE CÁLCULO DE LI, MERIFIELD Y LYAMIN"

TESINA DE GRADO

Previa a la obtención del Título de:

INGENIERO DE MINAS

Presentado por:

WILLIAM NABIL MOROCHO MONDAVÍ

GUAYAQUIL – ECUADOR

AÑO 2010

AGRADECIMIENTO

ING. JULIO JARAMILLO ROMERO
por su invaluable amistad, ánimo y guía para seguir esta noble carrera, así como su ayuda para elaborar este trabajo.

DEDICATORIA

A MIS AMADOS PADRES
WALTER Y SADYGHEH
Y MEMORIA DE MI ABUELO
LUIS

En tributo a sus abnegados esfuerzos
de toda una vida por educarme para el
servicio a la humanidad

TRIBUNAL DE GRADUACIÓN

Ing. Gastón Proaño Cadena

DECLARACIÓN EXPRESA

"La responsabilidad del contenido de esta Tesis de Grado, me corresponde exclusivamente; y el patrimonio intelectual de la misma a la Escuela Superior Politécnica del Litoral"

(Reglamento de Graduación de la ESPOL)

NABIL MOROCHO MONDAVÍ

RESUMEN

Una de las necesidades más apremiantes de la industria minera es la de maximizar el volumen de mineral explotable y al mismo tiempo realizar el proceso de extracción de manera segura y estable. En el caso de canteras, el volumen de mineral explotado se maximiza al aumentar la altura del talud. El desafío es, por lo tanto, el de determinar alturas seguras de taludes y al mismo tiempo económicamente aceptables.

El presente trabajo explora una metodología de trabajo para evaluar un macizo rocoso utilizando sistemas que tradicionalmente han demostrado validez y congruencia entre la teoría y la práctica, como es el caso de los sistemas de evaluación de macizos rocosos de Bieniawski y de Romana, este último aplicado a taludes especialmente.

Basado en los resultados obtenidos de los sistemas de evaluación de macizos rocosos antes mencionados, se realiza el cálculo del factor de seguridad utilizando un método sencillo basado en gráficos propuestos por un equipo de investigadores australianos, aplicado al caso de análisis de esta Tesina.

INDICE GENERAL

ABREVIATURAS

RMR.- Rock Mass Rating o Categorización de Macizo Rocoso

SMR.- Slope Mass Rating o Categorización de Macizo en Talud

RQD.- Rock Quality Designation o Factor de Calidad de Roca expresada en %

σ_{ci}.- resistencia a la compresión uniaxial de la roca intacta

β.- ángulo del talud (parámetro variable, iterativo, de máximo 75°)

H.- altura del talud (parámetro variable, iterativo)

GSI.- índice de resistencia geológica (grado de fracturación de la roca, calificado sobre 100)

m_i.- parámetro de cesión de la roca intacta

γ.- peso específico de la roca

N.- factor de estabilidad adimensional

INDICE DE TABLAS

INDICE DE GRÁFICOS

INTRODUCCIÓN

El presente trabajo tiene por objetivo realizar una evaluación de un macizo rocoso utilizando los métodos de evaluación de campo RMR de Bieniawski y SMR de Romana, puesto que ofrecen la comodidad de ser métodos visuales y que no incurren en significativos gasto para el análisis de la roca *in situ*; también estos métodos, particularmente el RMR, han resistido la imbatible prueba del tiempo al ofrecer resultados teóricos que han sido aplicados y corroborados en el campo con excelentes resultados.

En esta Tesina se introduce el trabajo realizado por Li, Merifield, y Lyamin, los dos primeros investigadores de University of Western Australia, y el último de University of New Castle – Australia. En su trabajo estos investigadores han realizado una serie de gráficos que sirven para realizar el análisis de estabilidad de taludes basados en las premisas de Hoek y Brown; estos gráficos simplifican en gran medida la laboriosa actividad de cálculo manual de estabilidad en macizos rocosos cuando no se dispone de programas informáticos que puedan hacerlo.

Finalmente, y como parte medular de este trabajo, se ha realizado el cálculo del factor de seguridad para taludes de las áreas mineras en cuestión. Puesto que las condiciones de la calidad del macizo rocoso cambian a lo largo de la cantera de andesita se ha realizado un análisis de algunos escenarios en donde se ha variado ciertos parámetros geotécnicos y observado el comportamiento de los resultados. Con esta información

en mano se ha graficado algunas curvas de factor de seguridad para la cantera, las mismas que se podrán utilizar para seleccionar una altura de banco de explotación seguro y al mismo tiempo económicamente factible para el proyecto minero.

CAPÍTULO I

Descripción geológico – geomecánica básica y ubicación del área de interés

Las áreas mineras "Victoria I" y "Victoria II" se encuentran emplazadas entre las formaciones "Yunguilla" y "Biblián". La formación "Yunguilla" tiene una inclinación hacia el occidente con afloramientos de 150 m a la altura del Tahual, aquí su litología es conformada por argilitas que pasan a arcillas. Su silicificación conlleva láminas carbonatadas. La formación "Biblián" tiene una potencia aproximada de 200 m. El macizo rocosa se encuentra muy fracturado presentando formación laminar y columnar. Esta formación descansa sobre la formación "Yunguilla". La conformación del cerro "Tahual" comprende tobas andesíticas, y es sobre esta formación donde se desarrollan las actividades mineras.

En general la andesita de esta zona ofrece una resistencia a la compresión de 98 Mega Pascal y un peso específico en seco de 2.5 toneladas por metro cúbico, porosidad 0.2%. Estas características la vuelven apta para el uso como agregado para hormigón que es propósito para el cual es usado actualmente.

CAPÍTULO II

Metodología propuesta para valorar un macizo rocoso geotécnicamente anisotrópico usando el sistema RMR y SMR

En la teoría, los sistemas de evaluación RMR de Bieniawski y SMR de Romana exigen realizar observaciones de ciertos rasgos particulares del macizo rocoso en zonas donde exista cierto grado de isotropía geotécnica; incluso, para ciertos parámetros de evaluación, se requiere realizar observaciones puntuales dentro del área de 1 metro cuadrado estándar dentro del cuerpo del macizo. Naturalmente en la práctica es muy difícil identificar y establecer con exactitud una sola zona con características geotécnicas similares, más aún cuando un mismo macizo rocoso puede estar formado por un conjunto de zonas con diferentes grados de meteorización, fracturación, orientación de diaclasas, etc., que vuelven al macizo geotécnicamente anisotrópico.

El caso del macizo rocoso de las áreas mineras "Victoria I" y "Victoria II" corresponde a un macizo altamente anisotrópico, lo que imposibilita realizar una evaluación en una sola zona del macizo para luego extrapolar los resultados de este análisis para todo el cuerpo rocoso.

Para resolver este inconveniente se ha desarrollado la siguiente metodología de campo para realizar una evaluación de un macizo rocoso geotécnicamente anisotrópico:

1. *Reconocimiento global del área de estudio.*- con esto se pudo determinar el aspecto general del macizo rocoso y obtener una primera idea de su calidad y posible comportamiento geotécnico: roturas planares, en cuña, etc.

2. *División del área de estudio en zonas de valoración.*- para esto se procedió a identificar zonas dentro del área de estudio que tuvieran características similares y preferentemente continuas, es decir, zonas donde las discontinuidades en las rocas tuvieran rumbos y buzamientos similares, el grado de meteorización sea aproximadamente homogéneo., etc. Estas zonas pueden considerarse como zonas de familias de discontinuidades similares.

3. *Medición de rumbos y buzamiento de las discontinuidades.*- utilizando el método clásico de mediciones con brújula

4. *Medición del espaciamiento entre discontinuidades.*- para esto se consideró un espaciamiento promedio *entre una discontinuidad y la siguiente* observadas en la zona de valoración.

5. *Conteo de discontinuidades en 1 metro cuadrado*.- este conteo del número de discontinuidades es necesario para la estimación del RQD de correlación; se seleccionó un área representativa dentro de la zona de valoración y se realizó el conteo por observación visual.

6. *Análisis del las condiciones de las discontinuidades*.- esto implica un reconocimiento del ancho de las grietas *entre* discontinuidades, material de relleno presente en las grietas, evidencia de meteorización, rugosidad de la grieta, etc.

7. *Identificación de presencia de agua*.- para esto se consideraron las condiciones de humedad que se observaron al momento de la visita de campo; además, se consideró hasta qué punto la topografía y suelo de la zona podría favorecer la conductividad hidráulica por escorrentía y filtración.

CAPÍTULO III

Recopilación de información de campo

Poniendo en práctica la metodología descrita en el numeral anterior, se procedió a realizar un reconocimiento del área de interés a evaluar, y se lo dividió en 3 zonas que ofrecían características isotrópicas regulares; si se necesitara realizar una evaluación similar en otra área se tendría nada más que dividirla en el número de zonas que resultaren necesarias para realizar observaciones de campo apropiadas.

A continuación se presenta los resultados obtenidos de las observaciones de campo:

TABLA 1. INFORMACIÓN RECOPILADA EN CAMPO

Zona	Rumbo	Buzamiento	Espaciado entre discontinuidades	Número de discontinuidades por m^2	Condición de las discontinuidades	Presencia de Agua
1	N 55 W	N 35 W	35 cm	7 horizontales 5 verticales TOTAL: 12	Grietas ligeramente rugosas. Paredes altamente meteorizadas.	Húmedo
2	N 30 W	S 70 E	15 cm	16 horizontales 10 verticales TOTAL: 26	Grietas pulidas , con separación de entre 1 a 5 mm.	Húmedo
3	S 20 E	S 80 W	30 cm	4 horizontales 2 verticales TOTAL: 6	Grietas ligeramente rugosas. Paredes altamente meteorizadas.	Húmedo

CAPÍTULO IV

Procesamiento de la información de campo y cálculos requeridos por los sistemas RMR y SMR

4.1 Sistema de evaluación RMR de Bieniawski

Como se ha mencionado repetidamente en este trabajo, se pretende hacer una valoración de la calidad del macizo rocoso utilizando el método RMR (*Rock Mass Rating*) desarrollado por Bieniawski (1972-'73). Este método tiene la gran particularidad de haber resistido la prueba del tiempo en cuanto a la precisión y calidad de los resultados que ofrece. Los parámetros que se consideran para este método son:

- Resistencia a la compresión uniaxial de la roca intacta, expresado en MPa.
- RQD (*Rock Quality Designation)*
- Espaciamiento entre discontinuidades
- Condiciones de las discontinuidades (estado de las grietas)
- Presencia de agua

Con excepción del RQD, todos los demás parámetros son datos recolectados en el campo. La estimación del RQD de correlación se obtiene utilizando la ecuación propuesta por Palmström (1982):

$$RQD = 115 - 3.3(Jv)$$

donde *Jv* es el número de discontinuidades por metro cuadrado, dato que se puede apreciar en la Tabla 1. En la siguiente Tabla se presentan los resultados de la estimación del RQD de correlación para cada una de las zonas de estudio:

TABLA 2. ESTIMACIÓN DEL RQD DE CORRELACIÓN	
Zona 1	75.4%
Zona 2	29.2%
Zona 3	95.2%

Con el valor del RQD de correlación calculado en la Tabla 2, es posible realizar la valoración utilizando el método de valoración RMR de Bieniawski, como se puede apreciar en la tabla a continuación, en la siguiente página:

TABLA 3. VALORACIÓN RMR DE BIENIAWSKI

	PARÁMETRO	VALOR	RESULTADO
ZONA 1	Resistencia de la Roca Intacta (MPa)	12	Puntaje Total: 69 Tipo de Roca: 2 Descripción: Buena
	RQD (%)	17	
	Espaciado de la discontinuidades (cm)	10	
	Condición de las discontinuidades	20	
	Presencia de agua	10	
ZONA 2	Resistencia de la Roca Intacta (MPa)	12	Puntaje Total: 48 Tipo de Roca: 3 Descripción: Regular
	RQD (%)	8	
	Espaciado de la discontinuidades (cm)	8	
	Condición de las discontinuidades	10	
	Presencia de agua	10	
ZONA 3	Resistencia de la Roca Intacta (MPa)	12	Puntaje Total: 72 Tipo de Roca: 2 Descripción: Buena
	RQD (%)	20	
	Espaciado de la discontinuidades (cm)	10	
	Condición de las discontinuidades	20	
	Presencia de agua	10	

Los resultados presentados en la Tabla 3 reflejan solamente la valoración RMR básica, sin considerar los factores de ajuste para taludes que se necesitan realizar y que dependen del rumbo y buzamiento de las discontinuidades.

4.2 Sistema de evaluación SMR de Romana

Este sistema de evaluación diseñado por Romana en 1995 introduce un conjunto de factores de análisis para adaptar el sistema de evaluación de Bieniawski a la evaluación de la calidad del macizo rocoso en taludes. Los parámetros considerados por Romana son:

- **F1**: relación entre el rumbo del talud (a_s) y el rumbo de las discontinuidades (a_j)
- **F2**: dependiente del buzamiento de la discontinuidades (b_j), suponiendo rotura planar
- **F3**: relación entre el buzamiento del talud (b_s) y el buzamiento de las discontinuidades (b_j)
- **F4**: factor empírico dependiente del método de excavación empleado

Así, la ecuación para realizar la valoración de taludes, según Romana es:

$$SMR = RMR + (F1 \times F2 \times F3) + F4$$

La información sobre rumbos y buzamientos de las zonas de valoración se encuentran en la Tabla 1. Con esta información se ha elaborado la siguiente tabla para obtener los valores de los factores de ajuste y el cálculo final del SMR para cada zona:

TABLA 4. VALORACIÓN SMR DE ROMANA

	FACTOR DE AJUSTE	VALOR	RESULTADO
ZONA 1	F1:$a_s - a_j$: *30° Favorable*	0.40	SMR = 69 -16.8 +8 = 60.2 Nuevo tipo de roca: 3 Descripción: Regular Estabilidad: Parcial
	F2: b_j : *35° Regular*	0.70	
	F3: $b_j - b_s$: *-48° Muy desfavorable*	-60	
	F4: Voladura ordinaria	8	
ZONA 2	F1:$a_s - a_j$: *55° Muy favorable*	0.15	SMR = 48 -0.56 +8 = 55.44 Nuevo tipo de roca: 3 Descripción: Regular Estabilidad: Parcial
	F2: b_j : *30° Muy favorable*	0.15	
	F3: $b_j - b_s$: *0° Regular*	-25	
	F4: Voladura ordinaria	8	
ZONA 3	F1:$a_s - a_j$: *5° Desfavorable*	0.85	SMR = 72 -23.15 +8 = 56.85 Nuevo tipo de roca: 3 Descripción: Regular Estabilidad: Parcial
	F2: b_j : *80° Muy desfavorable*	1.00	
	F3: $b_j - b_s$: *-3° Regular*	-25	
	F4: Voladura ordinaria	8	

CAPÍTULO V

Determinación de la altura óptima de banco para talud usando el método de cálculo del factor de seguridad de Li, Merifield, y Lyamin

5.1 Factor de seguridad

El factor de seguridad para taludes es una cifra adimensional que establece la relación existente entre las fuerzas que se oponen al deslizamiento frente a las fuerzas que favorecen el deslizamiento, desprendiéndose de esto que si el factor de seguridad es mayor a 1 el talud es estable.

$$\tilde{n}\, FS = \frac{\Sigma\ fuerzas\ opuestas\ al\ deslizamiento}{\Sigma\ fuerzas\ a\ favor\ del\ desplazamiento}$$

$$Si\ FS \leq 1\ entonces\ talud\ inestable$$
$$Si\ FS > 1\ entonces\ talud\ estable$$

Sin embargo, es necesario realizar una observación al respecto de esto último. El simple hecho de que el factor de seguridad sea ligeramente mayor a 1 y por ende se afirme que un talud es estable supone que las condiciones estáticas del talud son inalterables y constantes en el tiempo. En la práctica, en cualquier momento podría haber un cambio en el estado tensional – estático del macizo rocoso y podrían entonces aparecer nuevas fuerzas que favorezcan el deslizamiento. Por lo tanto, es necesario que el factor de seguridad sea mucho mayor a 1 para tener un margen de seguridad más amplio.

5.2 Cálculo de Factor de Seguridad utilizando el método de Li, Merifield, y Lyamin

La contribución realizada por Li, Merifield, y Lyamin resulta de la necesidad de tablas y curvas de estabilidad para macizos rocosos que permitan realizar estimaciones sencillas y correctas, sin necesidad de realizar extensas pruebas geomecánicas de rocas en laboratorio y sin utilizar matemáticas demasiado complejas. La única limitación de este trabajo es que parte de una altura de talud fija y luego determina el factor de seguridad.

El fundamento para este método de análisis está basado en el criterio de falla de Hoek – Brown que está apoyado en un sistema de clasificación denominado Índice de Resistencia Geológica o GSI (*Geological Stregnth Index*); este sistema de clasificación, que se introdujo para macizos rocoso altamente fracturados, resulta equivalente con el sistema de evaluación de Bieniawsky y ha sido una valiosa herramienta de ingeniería para estimación de resistencia y estabilidad de macizos rocosos.

Los parámetros que considera para el análisis son:

- σ_{ci}: resistencia a la compresión uniaxial de la roca intacta
- β: ángulo del talud (parámetro variable, iterativo, de máximo 75°)
- H: altura del talud (parámetro variable, iterativo)
- *GSI:* índice de resistencia geológica (grado de fracturación de la roca, calificado sobre 100)
- m_i: parámetro de cesión de la roca intacta
- γ: peso específico de la roca
- N: factor de estabilidad adimensional

De esta manera se pudo establecer una relación numérica inicial para determinar el factor de seguridad, y que obedece a la siguiente ecuación:

$$N = \frac{\sigma_{ci}}{\gamma H F}$$

También se desarrollaron una serie de gráficos que permiten obtener el valor de N utilizando una relación entre el valor del parámetro de cesión de la roca intacta m_i, y el valor de GSI. Se presenta a continuación el gráfico utilizado para este caso de estudio:

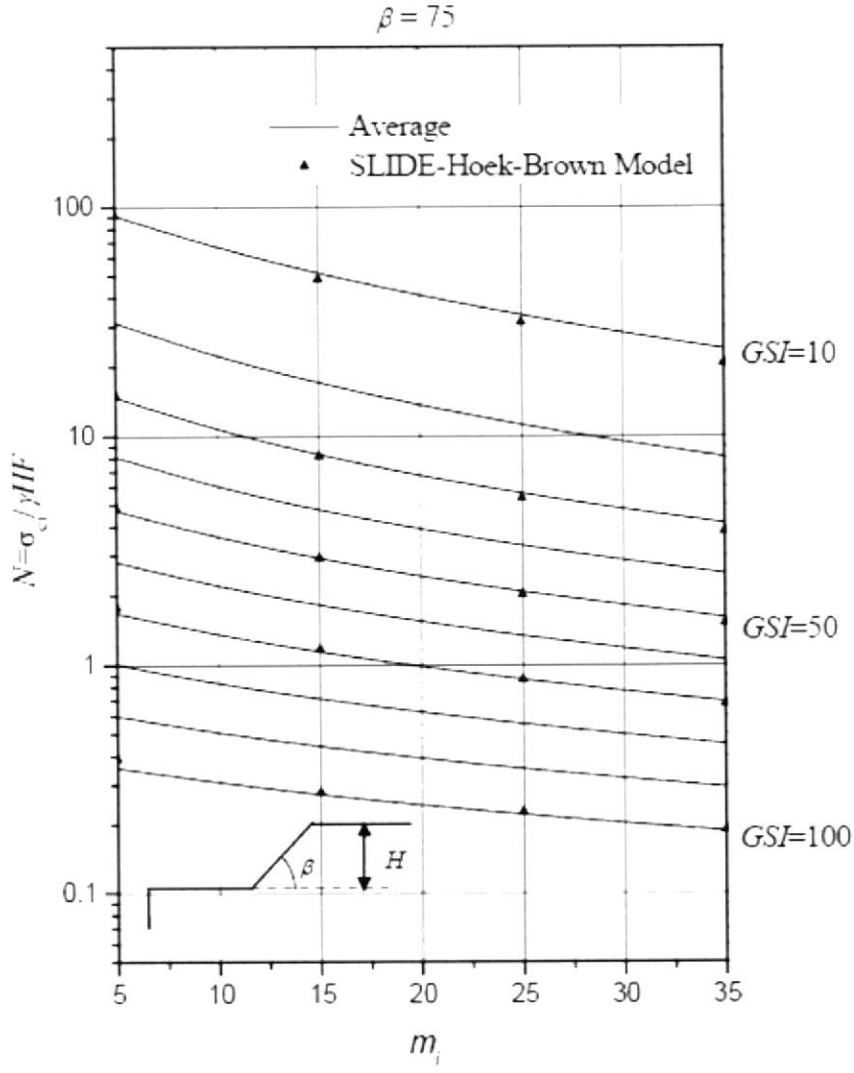

Gráfico 1.- *Relación entre GSI y m_i para obtención del valor N*

5.3 Aplicación al caso de estudio

El siguiente ejemplo se ha desarrollado para el caso de la cantera de andesita en las áreas mineras "Victoria I" y "Victoria II", donde se desea maximizar el ángulo y altura del talud para aumentar el volumen de mineral explotable.

Los datos disponibles para cálculo son:

- σ_{ci}: 98 MPa
- β: 75°, tomado para maximizar volumen posible de minado
- H: 1 metro, como base para modificación posterior
- GSI: 30, correspondiente a un macizo muy fracturado en bloques
- m_i: 19
- γ: 27 KN/m^3

Si por un momento se considera la condición ideal de equilibrio estático entre las fuerzas que actúan en el macizo rocoso, se podría asumir que F=1. Así, el valor equivalente de N para un bloque de roca intacto en condiciones ideales sería:

$$\frac{\sigma_{ci}}{\gamma H} = \frac{98000}{27 \times 1} = 3629{,}63$$

Sin embargo, del Gráfico 1 presentado en la sección anterior, se establece el valor de N basado en el GSI y el m_i.

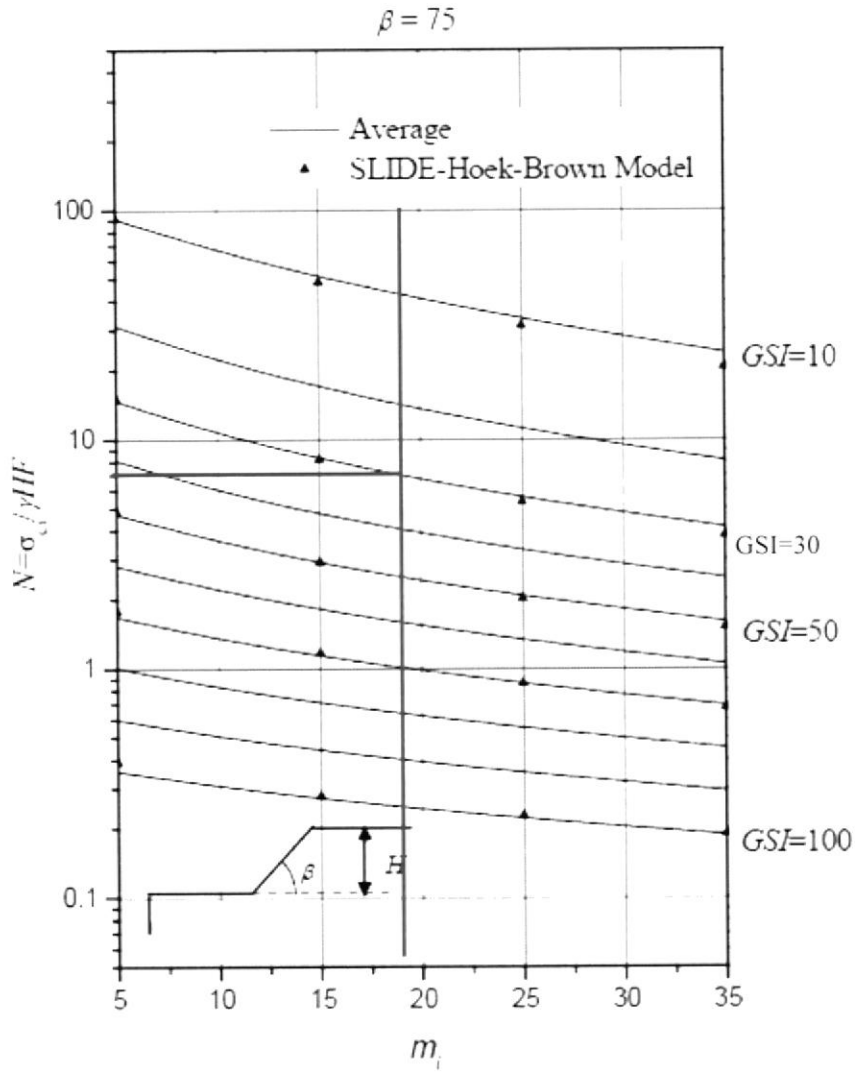

Así, el primer valor obtenido para N es igual a 7. Sustituyendo este valor en la ecuación original para N y despejando el valor del factor de seguridad F se tiene que:

$$F = \frac{\sigma_{ci}}{\gamma HN} = \frac{98000}{27 \times 1 \times 7} = 518.72$$

Es importante recordar que el parámetro variable para este caso es la altura: se desea determinar la altura máxima posible para el talud y que se encuentre al mismo tiempo dentro de un rango de seguridad determinado por F.

Lo que se propone ahora es establecer un valor límite inferior F de tal manera que se pueda concluir que la altura de talud H que generó ese valor de F es una altura de talud segura; no se puede considerar el valor de $F=1$ pues esto significaría que la condición de equilibrio estático es el ideal y que la más mínima variación de algún factor de estabilidad podría provocar un deslizamiento. Así el valor mínimo de F se propone que sea de 50, es decir, que las fuerzas que favorecerían el deslizamiento en un momento dado tendrían que ser 50 veces más grandes que las fuerzas que generan estabilidad.

Por lo tanto, se realizarán a continuación una serie de cálculos iterativos sencillos donde H es la variable independiente y F es la variable dependiente, con la particularidad de que mientras el valor de F no esté por debajo de un límite establecido entonces los valores de H son aceptables.

La ecuación sobre la cual ser realizará las iteraciones es:

$$F = \frac{\sigma_{ci}}{\gamma HN}$$

Para valores de H: 1, 2,3…n, tal que $F \geq 50$; γ: 27 KN/m^3; $N = 7$; σ_{ci}: 98 MPa

Iteración 0 – $H = 1$:

$$F = \frac{\sigma_{ci}}{\gamma HN} = \frac{98000}{27 \times 1 \times 7} = 518.72$$

Iteración 1 – $H = 2$:

$$F = \frac{\sigma_{ci}}{\gamma HN} = \frac{98000}{27 \times 2 \times 7} = 259.26$$

Iteración 2 – $H = 3$:

$$F = \frac{\sigma_{ci}}{\gamma HN} = \frac{98000}{27 \times 3 \times 7} = 172.84$$

Iteración 3 – $H = 4$:

$$F = \frac{\sigma_{ci}}{\gamma HN} = \frac{98000}{27 \times 4 \times 7} = 129.63$$

Iteración 4 – $H = 5$:

$$F = \frac{\sigma_{ci}}{\gamma HN} = \frac{98000}{27 \times 5 \times 7} = 103.70$$

Iteración 5 – $H = 6$:

$$F = \frac{\sigma_{ci}}{\gamma HN} = \frac{98000}{27 \times 6 \times 7} = 86.42$$

Iteración 6 – $H = 7$:

$$F = \frac{\sigma_{ci}}{\gamma HN} = \frac{98000}{27 \times 7 \times 7} = 74.07$$

Iteración 7 – $H = 8$:

$$F = \frac{\sigma_{cl}}{\gamma HN} = \frac{98000}{27 \times 8 \times 7} = 64.81$$

Iteración 8 – $H = 9$:

$$F = \frac{\sigma_{cl}}{\gamma HN} = \frac{98000}{27 \times 9 \times 7} = 57.61$$

Iteración 9 – $H = 10$:

$$F = \frac{\sigma_{cl}}{\gamma HN} = \frac{98000}{27 \times 10 \times 7} = 51.85$$

Iteración 10 – $H = 11$:

$$F = \frac{\sigma_{cl}}{\gamma HN} = \frac{98000}{27 \times 11 \times 7} = 47.14$$

Según lo propuesto anteriormente, se descarta la Iteración 10, pues el valor de F es 47.14 y por lo tanto menor a 50. Por lo tanto se considera los resultados obtenidos en la Iteración 9 donde el valor de F es de 51.85 generado por H de 10 metros. De esto se desprende que para las condiciones presentadas en este numeral la altura de talud apropiada es de 10 metros.

A continuación se presenta la curva de relación entre el valor de F y el valor de H que se desprende de las iteraciones antes presentadas:

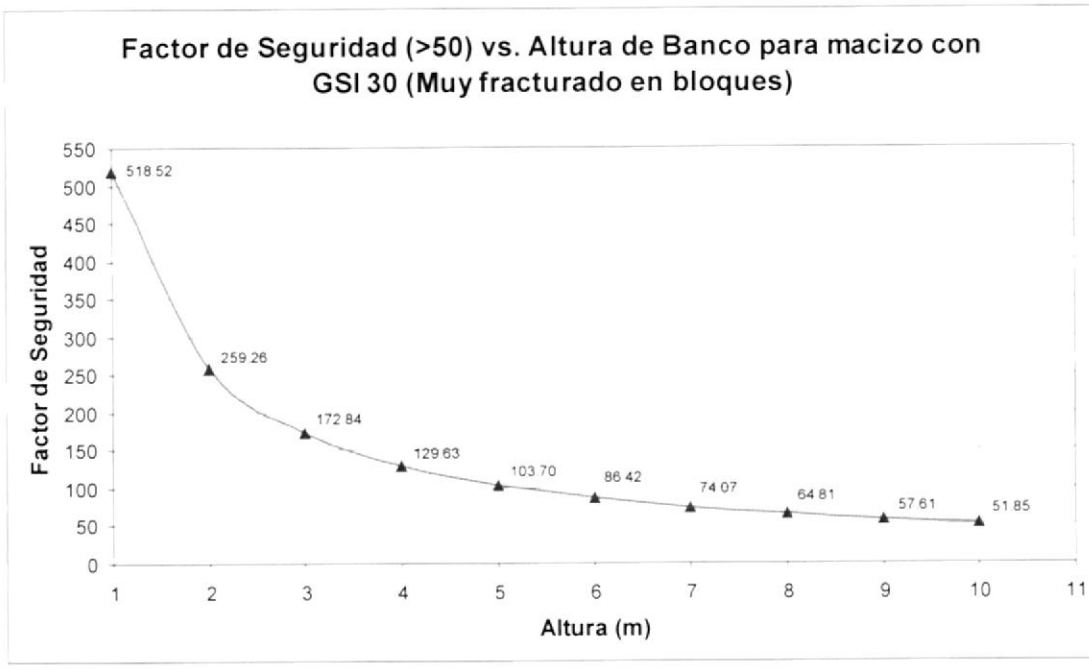

Gráfico 2.- *Relación entre los valores del Factor de Seguridad (F) y Altura (H) para un macizo con GSI 30*

Sin embargo, es necesario recordar que un macizo rocoso no tiene comportamiento isotrópico en toda su extensión y podrían existir variaciones en sus características geotécnicas y geológicas. Por lo tanto es necesario realizar un análisis posterior en donde las variaciones estarán determinadas por el parámetro de cesión de la roca intacta m_i y por el Índice de Resistencia Geológica *GSI*:

De las observaciones realizadas en el campo se ha establecido que el valor de m_i podría variar de entre 10, 15 y 19, y que el valor de *GSI* estaría entre 20 y 60, dependiendo del grado de fracturación de la roca. Los datos tabulados se muestran en las siguientes páginas.

También se ofrece un gráfico que muestra la relación entre el valor de F y de H si en la *GSI*.

TABLA 5.- ALTURAS DE BANCO SEGURAS DEPENDIENTES DE VARIACIONES EN *mi* Y *GSI*

mi=19 FACTOR DE SEGURIDAD PARA GSI:	mi= 15 FACTOR DE SEGURIDAD PARA GSI:	mi= 10 FACTOR DE SEGURIDAD PARA GSI:

Altura de banco	60	50	40	30	20	60	50	40	30	20	60	50	40	30	20
1	2016.46	1296.30	885.28	518.52	241.98	1728.40	1170.85	725.93	417.20	181.48	1578.10	930.67	558.40	329.97	157.81
2	1008.23	648.15	442.64	259.26	120.99	864.20	585.42	362.96	208.60	90.74	789.05	465.34	279.20	164.98	78.90
3	672.15	432.10	295.09	172.84	80.66	576.13	390.28	241.98	139.07	60.49	526.03	310.22	186.13	109.99	52.60
4	504.12	324.07	221.32	129.63	60.49	432.10	292.71	181.48	104.30	45.37	394.52	232.67	139.60	82.49	39.45
5	403.29	259.26	177.06	103.70	48.40	345.68	234.17	145.19	83.44	36.30	315.62	186.13	111.68	65.99	31.56
6	336.08	216.05	147.55	86.42	40.33	288.07	195.14	120.99	69.53	30.25	263.02	155.11	93.07	54.99	26.30
7	288.07	185.19	126.47	74.07	34.57	246.91	167.26	103.70	59.60	25.93	225.44	132.95	79.77	47.14	22.54
8	252.06	162.04	110.66	64.81	30.25	216.05	146.36	90.74	52.15	22.69	197.26	116.33	69.80	41.25	19.73
9	224.05	144.03	98.36	57.61	26.89	192.04	130.09	80.66	46.36	20.16	175.34	103.41	62.04	36.66	17.53
10	201.65	129.63	88.53	51.85	24.20	172.84	117.08	72.59	41.72	18.15	157.81	93.07	55.84	33.00	15.78
11	183.31	117.85	80.48	47.14	22.00	157.13	106.44	65.99	37.93	16.50	143.46	84.61	50.76	30.00	14.35
12	168.04	108.02	73.77	43.21	20.16	144.03	97.57	60.49	34.77	15.12	131.51	77.56	46.53	27.50	13.15
13	155.11	99.72	68.10	39.89	18.61	132.95	90.07	55.84	32.09	13.96	121.39	71.59	42.95	25.38	12.14
14	144.03	92.59	63.23	37.04	17.28	123.46	83.63	51.85	29.80	12.96	112.72	66.48	39.89	23.57	11.27
15	134.43	86.42	59.02	34.57	16.13	115.23	78.06	48.40	27.81	12.10	105.21	62.04	37.23	22.00	10.52
16	126.03	81.02	55.33	32.41	15.12	108.02	73.18	45.37	26.07	11.34	98.63	58.17	34.90	20.62	9.86
17	118.62	76.25	52.08	30.50	14.23	101.67	68.87	42.70	24.54	10.68	92.83	54.75	32.85	19.41	9.28
18	112.03	72.02	49.18	28.81	13.44	96.02	65.05	40.33	23.18	10.08	87.67	51.70	31.02	18.33	8.77
19	106.13	68.23	46.59	27.29	12.74	90.97	61.62	38.21	21.96	9.55	83.06	48.98	29.39	17.37	8.31
20	100.82	64.81	44.26	25.93	12.10	86.42	58.54	36.30	20.86	9.07	78.90	46.53	27.92	16.50	7.89
21	96.02	61.73	42.16	24.69	11.52	82.30	55.75	34.57	19.87	8.64	75.15	44.32	26.59	15.71	7.51
22	91.66	58.92	40.24	23.57	11.00	78.56	53.22	33.00	18.96	8.25	71.73	42.30	25.38	15.00	7.17
23	87.67	56.36	38.49	22.54	10.52	75.15	50.91	31.56	18.14	7.89	68.61	40.46	24.28	14.35	6.86
24	84.02	54.01	36.89	21.60	10.08	72.02	48.79	30.25	17.38	7.56	65.75	38.78	23.27	13.75	6.58
25	80.66	51.85	35.41	20.74	9.68	69.14	46.83	29.04	16.69	7.26	63.12	37.23	22.34	13.20	6.31
26	77.56	49.86	34.05	19.94	9.31	66.48	45.03	27.92	16.05	6.98	60.70	35.80	21.48	12.69	6.07
27	74.68	48.01	32.79	19.20	8.96	64.01	43.36	26.89	15.45	6.72	58.45	34.47	20.68	12.22	5.84
28	72.02	46.30	31.62	18.52	8.64	61.73	41.82	25.93	14.90	6.48	56.36	33.24	19.94	11.78	5.64
29	69.53	44.70	30.53	17.88	8.34	59.60	40.37	25.03	14.39	6.26	54.42	32.09	19.26	11.38	5.44
30	67.22	43.21	29.51	17.28	8.07	57.61	39.03	24.20	13.91	6.05	52.60	31.02	18.61	11.00	5.26
31	65.05	41.82	28.56	16.73	7.81	55.75	37.77	23.42	13.46	5.85	50.91	30.02	18.01	10.64	5.09
32	63.01	40.51	27.66	16.20	7.56	54.01	36.59	22.69	13.04	5.67	49.32	29.08	17.45	10.31	4.93

33	61.10	39.28	26.83	15.71	7.33	52.38	35.48	22.00	12.64	5.50	47.82	28.20	16.92	10.00	4.78
34	59.31	38.13	26.04	15.25	7.12	50.84	34.44	21.35	12.27	5.34	46.41	27.37	16.42	9.70	4.64
35	57.61	37.04	25.29	14.81	6.91	49.38	33.45	20.74	11.92	5.19	45.09	26.59	15.95	9.43	4.51
36	56.01	36.01	24.59	14.40	6.72	48.01	32.52	20.16	11.59	5.04	43.84	25.85	15.51	9.17	4.38
37	54.50	35.04	23.93	14.01	6.54	46.71	31.64	19.62	11.28	4.90	42.65	25.15	15.09	8.92	4.27
38	53.06	34.11	23.30	13.65	6.37	45.48	30.81	19.10	10.98	4.78	41.53	24.49	14.69	8.68	4.15
39	51.70	33.24	22.70	13.30	6.20	44.32	30.02	18.61	10.70	4.65	40.46	23.86	14.32	8.46	4.05
40	50.41	32.41	22.13	12.96	6.05	43.21	29.27	18.15	10.43	4.54	39.45	23.27	13.96	8.25	3.95
41	49.18	31.62	21.59	12.65	5.90	42.16	28.56	17.71	10.18	4.43	38.49	22.70	13.62	8.05	3.85
42	48.01	30.86	21.08	12.35	5.76	41.15	27.88	17.28	9.93	4.32	37.57	22.16	13.30	7.86	3.76
43	46.89	30.15	20.59	12.06	5.63	40.20	27.23	16.88	9.70	4.22	36.70	21.64	12.99	7.67	3.67

Nota: los valores coloreados corresponden a factores de seguridad inferiores a 50 y relacionados a alturas de banco no seguras

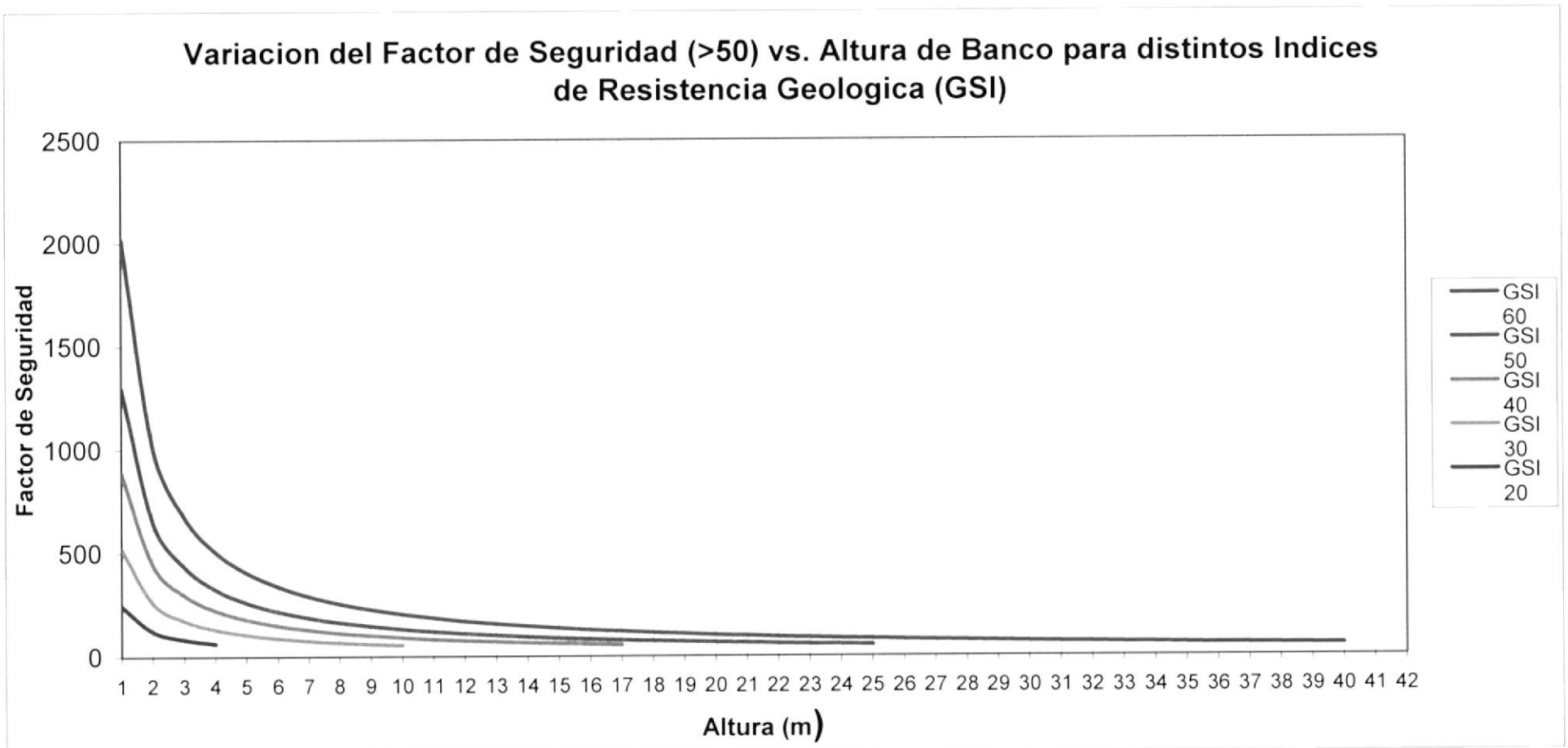

Gráfico 3.- *Relación entre los valores del Factor de Seguridad (F) y Altura (H) para el macizo rocoso considerando variaciones en el GSI*

CONCLUSIONES Y RECOMENDACIONES

De lo expuesto en la presente tesina es posible concluir que:

1. La metodología de evaluación de campo propuesta ofrece una forma ordenada para obtener información *in situ* que luego puede ser procesada para fines posteriores.

2. Existe una correlación lógica-empírica entre los resultados que ofrece la evaluación del macizo rocoso con los sistemas de Bieniawski y Romana y las aproximaciones gráfico-numéricas para determinación del Factor de Seguridad de Li, Merrifield y Lyman: el primer sistema de evaluación ofrece resultados cualitativos del macizo rocoso en términos de "muy malo, malo, regular, bueno, muy bueno" que lógicamente dan una base empírica para los resultados gráfico-numéricos del factor de seguridad.

3. Dada la correlación anteriormente descrita, es válido aseverar que ambos sistemas son mutuamente complementarios y por lo tanto esenciales al momento de determinar una altura segura de talud utilizando la metodología propuesta en esta tesina.

4. Los resultados finales obtenidos en la Tabla 5 , donde se ha variado el valor de m_i, y el *GSI*, ofrecen la versatilidad de proporcionar de manera rápida y segura una altura de banco apropiada para minado en cualquier momento en que, luego de una inspección visual, se determine que las condiciones de la roca en determinada zona del macizo han variado.

ANEXO UNICO

STABILITY CHARTS FOR ROCK SLOPES BASED ON THE HOEK-BROWN FAILURE CRITERION

A. J. Li [a], R. S. Merifield [b], A.V.Lyamin [c]

[a] Centre for Offshore Foundations Systems, The University of Western Australia, WA 6009, Australia
[b] Centre for Offshore Foundations Systems, The University of Western Australia, WA 6009, Australia
[c] Centre for Geotechnical and Materials Modelling, The University of Newcastle, NSW 2308, Australia

Tel: +61 8 6488 3141 Fax: +61 8 6488 1044

[a] email: anjui@civil.uwa.edu.au
[b] merifield@civil.uwa.edu.au
[c] andrei.lyamin@newcastle.edu.au

ABSTRACT

This paper uses numerical limit analysis to produce stability charts for rock slopes. These charts have been produced using the most recent version of the Hoek-Brown failure criterion. The applicability of this criterion is suited to isotropic and homogeneous intact rock or heavily jointed rock masses. The rigorous limit analysis results were found to bracket the true slope stability number to within $\pm 9\%$ or better and the difference in safety factor between bound solutions and limit equilibrium analyses using the same Hoek-Brown failure criterion is less than 4%. The accuracy of using equivalent Mohr-Coulomb parameters to estimate the stability number has also been investigated. For steep slopes, it was found using equivalent parameters produces poor estimates of safety factors and predictions of failure surface shapes. The reason for this lies in how these equivalent parameters are estimated, which is largely to do with estimating a suitable minor principal stress range. In order to obtain better equivalent parameter solutions, this paper proposes new equations for estimating the minor principal stress for steep and gentle slopes which can be used to determine equivalent Mohr-Coulomb parameters.

Keywords: Safety factor; Limit analysis; Rock; Slope stability; Failure criterion

1. Introduction

Predicting the stability of rock slopes is a classical problem for geotechnical engineers and also plays an important role when designing for dams, roads, tunnel and other engineering structures. Many researchers have focused on assessing the stability of rock slope [1-3]. However, the problem of rock slopes still presents a significant challenge to designers.

Stability charts for soil slopes were first produced by Taylor [4] and they continue to be used extensively as design tools and draw the attention of many investigators [1, 5].

Unfortunately, there are no such stability charts for rock slopes in the literature that are based on rock mass strength criteria. Although the stability charts proposed by Hoek and Bray [1] for Mohr-Coulomb material can be applied to rock or rockfill slopes, this requires knowledge of the equivalent Mohr-Coulomb cohesion and friction for the rock mass. Unfortunately, the strength of rock masses is notoriously difficult to assess. Nonetheless, many criteria have been proposed for estimating rock strength [6-10]. Currently, one widely accepted approach to estimating rock mass strength is the Hoek-Brown failure criterion [6, 11]. However, since most geotechnical software uses the Mohr-Coulomb failure criterion, stability chart solutions based on the Hoek-Brown yield criterion do not appear in the literature.

Generally speaking, rock masses are inhomogeneous, discontinuous media composed of rock material and naturally occurring discontinuities such as joints, fractures and bedding planes. These features make any analysis very difficult using simple theoretical solutions, like the limit equilibrium method. Moreover, without including special interface or joint elements, the displacement finite element method isn't suitable for analysing rock masses with fractures and discontinuities. Fortunately, the upper and lower bound formulations developed by Lyamin and Sloan [12, 13] and Krabbenhoft et al. [14] are ideally suited to modelling jointed or fissured materials because discontinuities exist inherently throughout the mesh. This feature was recently exploited by Sutcliffe et al. [15] and Merifield et al. [16] for predicting the bearing capacity of jointed rocks.

The purpose of this paper is to take advantage of the limit theorems ability to bracket the actual stability number of rock slopes. Both of the upper and lower bounds are employed to provide this set of stability charts. These solutions are obtained from numerical techniques developed by Lyamin and Sloan [12, 13] and Krabbenhoft et al.

[14] where the well-known Hoek-Brown yield criterion has been incorporated into limit analysis as presented by Merifield et al. [16].

As a means of comparison, the limit equilibrium method will then be used in conjunction with equivalent Mohr-Coulomb parameters for the rock and compared with the solutions obtained from the numerical limit analysis approaches. This will enable the validity of using equivalent Mohr-Coulomb parameters for rock slope calculations to be investigated.

2. Previous studies

The stability of rock slopes has attracted the attention of researchers for decades. In order to deal with the complications of rock slope failure mechanisms, Goodman and Kieffer [17] and Jaeger [18] outlined several simple methods and their limitations for estimating strength and stability of rock slopes. Due to the advancement of various computational techniques, our ability to more accurately evaluate rock slope stability and interpret the likely failure mechanisms has improved [19]. Buhan et al. [20] found that the final results of a stability analysis may be influenced by scale-effect of rock masses. Sonmez et al. [21] utilised back analysis of slope failures to obtain rock slope strength parameters. In their study, the applicability of rock mass classification, and a practical procedure of estimating the mobilised shear strength based on the Hoek-Brown yield criterion were explained. Previous investigations [22-25] of progressive failures and/or safety factor assessment of rock slopes have used a range of numerical methods. These include the continuum methods (finite element method and the finite difference method), the discontinuum methods (distinct element and discontinuous deformation analysis), and finite-/discrete-element codes. In addition, the probabilistic analytical method is employed by Yarahmadi Bafghi and Verdel [26] and Hack et al. [27] to find the rock slope potential failure key-group and estimate the probability of failure. It

should be acknowledged that the Slope Stability Probability Classification proposed by Hack et al. [27] does not require cohesion and friction as input. Yang et al. [28-30] adopt tangential strength parameters (c and ϕ) from the Hoek-Brown failure criterion in an upper bound analysis to obtain the optimised height of a slope. As far as the authors are aware, the studies of Yang et al. [28-30] represent the only attempt at providing slope stability factors for estimating rock slope stability.

Currently, practising engineers typically use a number of stability charts when attempting to predict the stability of rock slopes: (1) Hoek–Bray [1] charts can be used for rock and rockfill slopes; (2) Zanbak [31] proposed a set of stability charts for rock slopes susceptible to toppling; (3) Stability charts presented by Siad [32] based on the upper bound approach that can be used for rock slopes with earthquake effects. However, these three sets of design charts require conventional Mohr-Coulomb soil parameters, cohesion (c) and friction angle (ϕ), as input. From a review of literature, the authors are not aware of any slope stability chart solutions based on the native form of the Hoek-Brown failure criterion that require Hoek-Brown material parameters as input. This paper is concerned with providing a set of stability charts for rock slopes based on the Hoek-Brown failure criterion that can be used by practising engineers to rapidly assess the preliminary stability of rock slopes.

3. The generalised Hoek-Brown failure criterion

3.1 Applicability

Practitioners are often required to predict the strength of large-scale rock masses for design. Fortunately, Hoek and Brown [6] proposed an empirical failure criterion which developed through curve-fitting of triaxial test data suited for intact rock and jointed rock masses. The criterion is based on a classification system called the Geological Strength Index (GSI). The Hoek-Brown criterion is one of the few nonlinear criteria

widely accepted and used by engineers to estimate the strength of a rock mass. Therefore, it is appropriate to use this criterion when assessing the stability of istopic rock slopes in this study.

The *GSI* classification system is based upon the assumption that the rock mass contains sufficient number of ''randomly'' oriented discontinuities such that it behaves as an isotropic mass. In other words, the behaviour of the rock mass is independent of the direction of the applied loads. Therefore, it is clear that the *GSI* system should not be applied to those rock masses in which there is a clearly defined dominant structural orientation that will lead to highly anisotropic mechanical behaviour. In addition, it is also inappropriate to assign *GSI* values to excavated faces in strong hard rock with a few discontinuities spaced at distances of similar magnitude to the dimensions of slope under consideration. In such cases the stability of the slope will be controlled by the three-dimensional geometry of the intersecting discontinuities and the free faces created by the excavation.

In line with the above discussion, it is important to realise the stability charts presented in this paper will be subject to the same limitations that underpin the Hoek-Brown yield criterion itself. An excellent overview of the applicability and limitations of the *GSI* system can be found in Marinos et al [33].

An explanation for the applicability of Hoek-Brown criterion when applied to rock slopes is displayed in Fig. 1. After Hoek [34], for the same rock properties throughout the slope, rock masses can be classified into three structural groups, namely **GROUP I**, **GROUP II**, and **GROUP III**. Fig 1 shows the transition from an isotropic intact rock (**GROUP I**), through a highly anisotropic rock mass (**GROUP II**), to a heavily jointed rock mass (**GROUP III**). In this paper the rock slope has been assumed as either (1) intact or; (2) heavily jointed so that, on the scale of the problem, it can be regarded as an

isotropic assembly of interlocking particles. In the case of intact rock (**GROUP I**), it should be noted that the failure mechanism of intact rock may be brittle rather than plastic so the theories of plasticity may not be appropriate.

3.2 Numerical implementation

The upper bound and lower bound methods developed by Lyamin and Sloan [12, 13] and Krabbenhoft et al. [14] can deal with a wide range of yield criteria, however on deviatoric planes the surfaces of those criteria must be convex and smooth. The Hoek-Brown yield surface has apex and corner singularities in stress space, and therefore numerical smoothing is required to avoid singularities. Details of the implementation of the Hoek-Brown criterion into the numerical limit analysis formulations can be found in Merifield et al. [16] and will not be repeated here. In this study, the latest version of Hoek-Brown failure criterion [11] is employed. The Hoek-Brown criterion was first proposed in 1980 [6] and updated several times. The latest version used in this study is given by the following equation.

$$\sigma_1' = \sigma_3' + \sigma_{ci}\left(m_b\frac{\sigma_3'}{\sigma_{ci}} + s\right)^{\alpha} \tag{1}$$

Where

$$m_b = m_i \exp\left(\frac{GSI-100}{28-14D}\right) \tag{2}$$

$$s = \exp\left(\frac{GSI-100}{9-3D}\right) \tag{3}$$

$$\alpha = \frac{1}{2} + \frac{1}{6}\left(e^{-GSI/15} - e^{-20/3}\right) \tag{4}$$

The GSI was introduced because Bieniawski's rock mass rating RMR system [35] and the Q-system [36] were deemed to be unsuitable for poor rock masses. The GSI ranges

from about 10, for extremely poor rock masses, to 100 for intact rock. The parameter D is a factor that depends on the degree of disturbance. The suggested value of disturbance factor is $D = 0$ for undisturbed in situ rock masses and $D = 1$ for disturbed rock mass properties. The magnitude of the disturbance factor is affected by blast damage and stress relief due to overburden removal. For the analyses presented here, a value of $D = 0$ has been adopted.

The uniaxial compressive strength is obtained by setting $\sigma_3 = 0$ in Eq. (1), giving

$$\sigma_c = \sigma_{ci}\, s^{\alpha} \tag{5}$$

and the tensile strength is

$$\sigma_t = -\frac{s\,\sigma_{ci}}{m_b} \tag{6}$$

3.3 Equivalent Mohr-Coulomb parameters

Since most geotechnical engineering software is still written in terms of the Mohr-Coulomb failure criterion, it is necessary for practising engineers to determine equivalent friction angles and cohesive strengths for each rock mass and stress range. In the context of this paper, the solutions obtained by using equivalent Mohr-Coulomb parameters can be compared directly with the solutions from using the native Hoek-Brown failure criterion.

Fig. 2 is an illustration of the Hoek-Brown criterion and equivalent Mohr-Coulomb envelope. Because the equivalent Mohr-Coulomb envelope is a straight line, it can not fit the Hoek-Brown curve completely. If we divide Fig. 2 into three zones, namely **REGION 1**, **REGION 2**, and **REGION 3**, it can be seen that when rock stress conditions fall in **REGION 1** and **REGION 3**, using equivalent Mohr-Coulomb parameters may overestimate the ultimate shear strength when compared to the Hoek-

Brown curve. Regarding the fitting process, more details can be found in Hoek et al. [11] where the process involves balancing the areas above and below the Mohr-Coulomb plot over a range of minor principal stress values. This results in the following equations for friction angle and cohesive strength:

$$c' = \frac{\sigma_{ci}\left[(1+2\alpha)s+(1-\alpha)m_b\,\sigma'_{3n}\right]\left(s+m_b\,\sigma'_{3n}\right)^{\alpha-1}}{(1+\alpha)(2+\alpha)\sqrt{1+\left(6\alpha\,m_b\left(s+m_b\,\sigma'_{3n}\right)^{\alpha-1}\right)/(1+\alpha)(2+\alpha)}} \tag{7}$$

$$\phi' = \sin^{-1}\left[\frac{6\alpha\,m_b\left(s+m_b\,\sigma'_{3n}\right)^{\alpha-1}}{2(1+\alpha)(2+\alpha)+6\alpha\,m_b\left(s+m_b\,\sigma'_{3n}\right)^{\alpha-1}}\right] \tag{8}$$

where $\sigma_{3n} = \sigma'_{3\max}/\sigma_{ci}$.

It should be noted that the value of $\sigma'_{3\max}$ has to be determined for each particular problem. For slope stability problems, Hoek et al. [11] suggests $\sigma'_{3\max}$ can be estimated by the following equation:

$$\frac{\sigma'_{3\max}}{\sigma'_{cm}} = 0.72\left[\frac{\sigma'_{cm}}{\gamma H}\right]^{-0.91} \tag{9}$$

in which H is the height of the slope and γ is the material unit weight. For the stress range, $\sigma_t < \sigma'_3 < \sigma_{ci}/4$, the compressive strength of the rock mass σ'_{cm} can be determined as:

$$\sigma'_{cm} = \sigma_{ci}\frac{\left(m_b+4s-\alpha\left(m_b-8s\right)\right)\left(m_b/4+s\right)^{\alpha-1}}{2(1+\alpha)(2+\alpha)} \tag{10}$$

4. Problem definition

A plane strain illustration of the slope stability problem is shown in Fig. 3 where the jointed rock mass has an intact uniaxial compressive strength σ_{ci}, geological strength index GSI, intact rock yield parameter m_i, and unit weight γ. The rock weight γ can

be estimated from core samples and σ_{ci} and m_i can be obtained from either triaxial test results or from the tables proposed in Hoek [37]. Several approaches can be used to evaluate GSI as outlined by Hoek [37], which include using table solutions and estimating by using the rock mass rating (RMR) [35]. Excavated slope and tunnel faces are probably the most reliable source of information for GSI estimates. Hoek and Brown [38] also pointed out that GSI can be adjusted to a smaller magnitude in order to incorporate the effects of surface weathering. Greater detail on how to best estimate the Hoek-Brown material parameters can be found in Hoek and Brown [38], Hoek [37] and Wyllie and Mah [3].

In this study, all the quantities are assumed constant throughout the slope. In the limit analyses, for given slope geometry (H, β) and rock mass (σ_{ci} GSI, m_i), the optimized solutions of the upper bound and lower bound programs can be carried out with respect to the unit weight (γ). In this study, slope inclinations of $\beta = 15^\circ, 30^\circ, 45^\circ, 60^\circ$, and 75° are analysed. The effect of depth factor (d/H) was found to be insignificant. With the exception of the case where $\beta = 15^\circ$, all analyses indicated the primary failure mode was one where the slip line passed through the toe of the slope (Toe failure). The dimensionless stability number is defined as Eq. (11).

$$N = \frac{\sigma_{ci}}{\gamma H F} \tag{11}$$

where F is the safety factor of the slope.

5. Results and discussion of limit analyses

5.1 Limit analysis solutions

Figs. 4-8 present stability charts from the numerical upper and lower bound formulations for angles of $\beta = 15^\circ$ - 75° for a range of GSI and m_i. The stability

number N was defined in Eq. (11). Referring to Fig. 4, it is apparent that the upper and lower bound results bracket a narrow range of stability numbers N for $GSI = 10$, so an average value from the bound solutions could be adopted for simplicity. In fact, it was found that, for all the analyses performed, the range between upper and lower bound stability numbers was always less than $\pm 5\%$. The only exception to this observation occurs for the cases of $\beta = 45^{\circ}$ and low GSI values, where the range is around $\pm 9\%$. Therefore, average values of the stability number N have been adopted and presented unless stated otherwise. The parameter N can be seen to decrease as the value of GSI or m_i increases.

Figs. 9 and 10 show an alternative form of stability charts as a function of the slope angle (β). The users only need to estimate GSI and m_i for the rock mass, and then the stability number can be estimated for a given slope angle. For the same rock slope material, the differences in stability number between various slope angles can provide a ratio of safety factor. For example, it can be found that decreasing slope angles from $\beta = 75^{\circ}$ to $\beta = 60^{\circ}$ for $GSI = 80$ can increase the factor of safety by more than 50%.

Referring to the above results, for any given rock mass (σ_{ci}, GSI, m_i) and unit weight of the material γ, the obtained stability number can be used to determine the ultimate height of cut slopes. In addition, the charts indicate that the stability number N increases with increasing slope angle for a given GSI and m_i.

Fig. 11 displays several of the observed upper bound plastic zones for different slope angles in which $H = 1$. The depth of failure surface increases with the reduction of the slope angle. But this variation can not be found when the slope angle $\beta > 45^{\circ}$. For a given GSI, it was found that the depth of plastic zone is almost unchanged with increasing m_i.

5.2 Application example

The stability charts illustrated in Fig. 4-8 provide an efficient method to determine the factor of safety (F) for a rock slope. The following example is of a slope constructed in a very poor quality rock mass. It has the following parameters: the slope angle $\beta = 60^{\circ}$, the height of the slope $H = 25m$, the intact uniaxial compressive strength $\sigma_{ci} = 20MPa$, geological strength index $GSI = 30$, intact rock yield parameter $m_i = 8$, and unit weight of rock mass $\gamma = 23kN/m^3$. With this information, the safety factor (F) of this rock slope can be obtained using the following procedure:

From the values of σ_{ci}, γ and H, we can calculate a dimensionless parameter $\sigma_{ci}/\gamma H = 20000/(23 \times 25) = 34.8$.

In Fig. 7, $N = \sigma_{ci}/\gamma HF \approx 4$.

The factor of safety can be calculated as $F = 34.8/4 = 8.7$.

6. Results and discussion of limit equilibrium analyses

In general, rock slope stability is more often analysed using the limit equilibrium method and equivalent Mohr-Coulomb parameters as determined by Eq. (7) and Eq. (8). With this being the case, an obvious question is how do the limit equilibrium results using equivalent Mohr-Coulomb parameters compare to the limit analysis results using the Hoek-Brown criterion. In order to make this comparison, the commercial limit equilibrium software **SLIDE** [39] and Bishop's simplified method [40] have been used. The software **SLIDE** can perform a slope analysis using the Mohr-Coulomb yield or the generalised Hoek-Brown criterion. When the Mohr-Coulomb criterion is used, the cohesion (c) and friction angle (ϕ) are constant along any given slip surface and are independent of the normal stress as expected. However, when the Hoek-Brown criterion is selected, the software will calculate a set of instantaneous equivalent Mohr-Coulomb

parameters when analysing the slope based on the normal stress at the base of each individual slice. More details on how the parameters are actually calculated can be found in Hoek [37]. Therefore the cohesion (c) and the friction angle (ϕ) will vary along any given slip surface. By calculating equivalent Mohr-Coulomb parameters in this way, a more accurate representation of the curved nature of the Hoek-Brown criterion in τ - σ_n space is obtained. Referring to the Figs. 4-8, the triangular points shown represent the stability numbers obtained from the limit equilibrium method based on the Hoek-Brown strength parameters. It can be found that these points are remarkably close to the average lines of the limit analysis solutions and most of them locate between the upper and lower bound solutions.

For the given materials and geometrical properties of the slope, the finite element lower bound analysis will provide the optimum unit weight (γ) such that collapse has just occurred (i.e. Factor of safety $F = 1$). A critical non-dimensional parameter $(\sigma_{ci}/\gamma H)_{crit}$ can then be defined for the subsequent **SLIDE** analyses. In Table 1, the safety factor ($F1$) and ($F2$) are obtained using the Hoek-Brown criterion and the Mohr-Coulomb criterion in **SLIDE**, respectively. Both of these analyses are based on equivalent Mohr-Coulomb parameters with the only difference being how these parameters are calculated (as discussed above).

The comparisons of the safety factors F , $F1$ and $F2$ are shown in Table 1 where the largest difference between F and $F1$ and F and $F2$ are about 4% and 64%, respectively. This shows that the results of **SLIDE** analyses using the Hoek-Brown model compare well with the results of the lower bound limit analyses. In contrast the results of **SLIDE** analyses using the Mohr-Coulomb model do not compare favourably with the lower bound results. From Table 1, it can be found that using the Mohr-Coulomb model may lead to significant overestimations of safety factors, particularly

for steep slopes. The average difference between F and $F2$ for $\beta = 60^{\circ}$ and $\beta = 75^{\circ}$ was found to be 16.8% and 34.3% respectively. For all the cases, the average overestimation is 12.8%. It should be stressed that, a high estimation of safety factor will induce a non-conservative design. It was found that using the Hoek-Brown model in **SLIDE** will produce a failure mechanism in good agreement with the upper bound mechanism. The same could not be said when using the Mohr-Coulomb model. For $\beta = 30^{\circ}$, both of the two above models achieve similar failure surfaces which agree well with the upper bound plastic zone. In almost all cases, a toe-failure mode was observed, the only exception is the case of $\beta = 15^{\circ}$ (base-failure).

In order to determine the source of overestimations in factors of safety ($F2$) for steep slopes, the stress conditions on each slice from the **SLIDE** limit equilibrium analyses were observed more closely. It was found that, for steep slopes, the stress conditions of the slices along the failure plane tend to be located in **REGION 1** (Fig. 2) where the shape of the Hoek-Brown and Mohr-Coulomb strength criterions differs the greatest. In this region, at the same normal stress, the ultimate shear strength using the Hoek-Brown criterion is smaller than that of the Mohr-Coulomb criterion. Therefore, it is reasonable to conclude that using the equivalent Mohr-Coulomb parameters will provide a higher estimate of the safety factor.

From the results of this study, it appears that the equivalent parameters (c and ϕ) obtained from Eqs. (7)-(10) will lead to an unconservative factor of safety estimate, particular for steep slopes where $\beta \geq 45^{\circ}$. In order to improve the estimate of $F2$, it becomes apparent a better estimate of $\sigma_{3\max}^{'}$, and therefore a different form to Eq. (9), is required.

To determine a more appropriate value of $\sigma_{3\max}^{'}$ to be used in Eq. (7) and Eq. (8), a similar study as performed by Hoek et al. [11] is conducted. In these studies, Bishop's simplified method and **SLIDE** is used to analyse the cases in Table 1. For a factor of safety of 1, the relationship between $\sigma_{cm}^{'}/\gamma H$ and $\sigma_{3\max}^{'}/\sigma_{cm}^{'}$ is as illustrated in Fig. 12 and Fig. 13. The authors have tried to fit only one equation incorporating all data to replace Eq. (9), but this did not prove possible. Instead separate equations are presented for what is defined as steep slopes $\beta \geq 45^{\circ}$ and gentle slopes $\beta < 45^{\circ}$ as Eqs. (12) and (13) respectively.

$$\frac{\sigma_{3\max}^{'}}{\sigma_{cm}^{'}} = 0.2\left[\frac{\sigma_{cm}^{'}}{\gamma H}\right]^{-1.07} \quad (\text{Steep slope } \beta \geq 45^{\circ}) \tag{12}$$

$$\frac{\sigma_{3\max}^{'}}{\sigma_{cm}^{'}} = 0.41\left[\frac{\sigma_{cm}^{'}}{\gamma H}\right]^{-1.23} \quad (\text{Gentle slope } \beta < 45^{\circ}) \tag{13}$$

It can be seen in Fig. 12 and Fig. 13 the newly fitted Eq. (12) for steep slopes plots below the original Eq. (9) and the newly proposed Eq. (13) for gentle slopes plots above the original Eq. (9). For this reason, it is apparent that one curve fit is not possible for all slope angles.

In Table 1, the safety factors $F3$ and $F4$ are obtained from **SLIDE** using Mohr-Coulomb parameters which are calculated by estimating $\sigma_{3\max}^{'}$ from Eq. (12) and Eq. (13). Comparing $F3$ and $F4$ with $F2$, shows that for steep slope, the safety factors estimates are much improved. A summary of the results in Table 1 shows that, using newly proposed equations to calculate the equivalent Mohr-coulomb parameters, the largest difference of safety factor has decreased from 64% to 21% and the average difference has reduced from 12.8% to 3.4%. Thus, it can be concluded that using the modified Eq. (12) and Eq. (13) will provide better results of safety factors which are on

average only 3.4% higher than the lower bound results. The newly proposed Eq. (12) and Eq. (13) are both applicable in estimating $\sigma_{3\max}^{'}$ for $\beta = 45^{\circ}$ cases. The results show that the difference in safety factor between these two equations is less than 8%. This would be acceptable for preliminary assessment of rock slope stability.

Fig. 14 displays the upper bound plastic zones compared with failure surfaces obtained using **SLIDE** and different strength parameters from Eq. (12) and Eq. (13). $F1$, $F2$, and $F3$ denote the safety factors obtained from using the Hoek-Brown (σ_{ci}, GSI, m_i, D), the original equivalent Mohr-Coulomb (proposed by Hoek), and the new equivalent Mohr-Coulomb (proposed in this paper) strength parameters, respectively. It is shown that using the original estimated Mohr-Coulomb parameters in analyses gives poor assessment of the stability and predictions of failure surfaces for steep slopes. On the other hand, by using the new proposed equivalent Mohr-Coulomb parameters the predicted failure mechanism compares more favourably to the upper bound mechanism and the factor of safety is much improved.

7. Conclusions

Stability charts based on the Hoek-Brown failure criterion are presented using formulations of the upper and lower bound limit theorems. These chart solutions can be used for estimating rock slope stability for preliminary design. It is important that users understand the assumptions and limitations before using these new rock slope stability charts. In particular, it should be noted that the chart solutions proposed in this paper are applicable to isotropic rock or rock masses only. Regarding the results of this study, the following conclusions can be made:

The upper bound and lower bound solutions bracket a narrow range of stability numbers (N) within $\pm 9\%$ or better (i.e. $\pm 5\%$) for all cases. This provides confidence that the true stability number has been bracketed accurately.

The general mode of failure for rock slopes was observed to be of the toe-failure type, except for the case of $\beta = 15^{\circ}$, where a base-failure type was observed.

The accuracy of using equivalent Mohr-Coulomb parameters for the rock mass in a traditional limit equilibrium method of slice analysis has been investigated. It was found that the factor of safety can be overestimated by up to 64% for steep slopes if existing guidelines for equivalent parameter determination are used. In order to improve the factor of safety estimate, two modified equations for steep and gentle slopes have been proposed. These equations are modifications of those originally proposed by Hoek [11]. When they are used to determine equivalent Mohr-Coulomb parameters that are subsequently used in a method of slice analysis, the factor of safety estimate is much improved and is at most 21% above the limit analysis result.

It was found that a limit equilibrium method of slice analysis can be used in conjunction with equivalent Mohr-Coulomb parameters to produce factor of safety estimates close to the limit analysis results, provided modifications are made to the underlying formulations. Such modifications have been made in the software **SLIDE** where a set of equivalent Mohr-Coulomb parameters are calculated at the base of each individual slice. This approach predicts factors of safety remarkably close to the limit analysis solutions that are based on the native form of the Hoek-Brown criterion.

References

[1] Hoek E, Bray JW, Rock slope engineering. 3rd ed. London: Institute of Mining and Metallurgy, 1981.

[2] Goodman RE, Introduction to rock Mechanics. 2nd ed. New York: Wiley, 1989.

[3] Wyllie DC, Mah CW, Rock slope engineering. 4th ed. London; New York: Spon Press, 2004.

[4] Taylor DW, Stability of earth slopes. J. Boston Soc. Civ. Engrs. 1937;24:197-246.

[5] Gens A, Hutchinson JN, Cavounidis S, Three-dimensional analysis of slides in cohesive soils. Geotechnique 1988;38(1):1-23.

[6] Hoek E, Brown ET, Empirical strength criterion for rock masses. J. Geotech. Engng Div., ASCE 1980;106(9):1013-1035.

[7] Yu MH, Zan YW, Zhao J, Yoshimine M, A unified strength criterion for rock material. International Journal of Rock Mechanics & Mining Science 2002;39:975-989.

[8] Grasselli G, Egger P, Constitutive law for the shear strength of rock joints based on three-dimensional surface parameters. International Journal of Rock Mechanics & Mining Science 2003;40:25-40.

[9] Sheorey PR, Empirical rock failure criteria. Rotterdam, Netherlands: A. A. Balkema, 1997.

[10] Yudhbir, Lemanza W, Prinzl F. An empirical failure criterion for rock masses. In Proceedings of fifth congress of ISRM. 1983.

[11] Hoek E, Carranza-Torres C, Corkum B. Hoek-Brown Failure criterion-2002 edition. In Proceedings of the North American rock mechanics society meeting in Toronto. 2002.

[12] Lyamin AV, Sloan SW, Upper bound limit analysis using linear finite elements and non-linear programming. International Journal for Numerical and Analytical Methods in Geomechanics 2002;26:181-216.

[13] Lyamin AV, Sloan SW, Lower bound limit analysis using non-linear programming. International Journal for Numerical Methods in Engineering 2002;55:573-611.

[14] Krabbenhoft K, Lyamin AV, Hjiaj M, Sloan SW, A new discontinuous upper bound limit analysis formulation. International Journal for Numerical Methods in Engineering 2005;63:1069-1088.

[15] Sutcliffe DJ, Yu HS, Sloan SW, Lower bound solutions for bearing capacity of jointed rock. Computer and Geotechnics 2004;31:23-36.

[16] Merifield RS, Lyamin AV, Sloan SW, Limit analysis solutions for the bearing capacity of rock masses using the generalised Hoek-Brown criterion. International Journal of Rock Mechanics & Mining Sciences 2006;43:920-937.

[17] Goodman RE, Kieffer DS, Behavior of rock in slope. Journal of Geotechnical and Geoenviromental Engineering 2000;126(8):675-684.

[18] Jaeger JC, Friction of rocks and stability of rock slopes. Geotechnique 1971;21(2):97-134.

[19] Stead D, Coggan JS, Eberhardt E, Realistic simulation of rock slope failure mechanisms: The need to incoporate principles of failure mechanisms. International Journal of Rock Mechanics & Mining Science 2004;41 (3):2B 17-22.

[20] Buhan PD, Freard J, Garnier D, Maghous S, Failure properties of fractured rock masses as anisotropic homogenized media. Journal of Engineering Mechanics 2002;128(8):869-875.

[21] Sonmez H, Ulusay R, Gokceoglu C, A practical procedure for the back analysis of slope failures in closely jointed rock masses. International Journal of Rock Mechanics & Mining Science 1998;35(2):219-233.

[22] Hoek E, Read J, Karzulovic A, Chenn ZY. Rock slopes in civil and mining engineering. In Proceedings of the International Conference on Geotechnical and Geological Engineering. 2000, Melbourne.

[23] Wang C, Tannant DD, Lilly PA, Numerical analysis of stability of heavily jointed rock slopes using PFC2D. International Journal of Rock Mechanics & Mining Sciences 2003;40:415-424.

[24] Eberhardt E, Stead D, Coggan JS, Numerical analysis of initiation and progressive failure in natural rock slopes— the 1991 Randa rockslide. International Journal of Rock Mechanics & Mining Science 2004;41:69-87.

[25] Stead D, Eberhardt E, Coggan JS, Developments in the characterization of complex rock slope deformation and failure using numerical modelling techniques. Engineering Geology 2006;83:217-235.

[26] Yarahmadi Bafghi AR, Verdel T, Sarma-based key-group method for rock slope reliability analyses. International Journal for Numerical and Analytical Methods in Geomechanics 2005;29:1019-1043.

[27] Hack R, Price D, Rengers N, A new approach to rock slope stability - a probability classification (SSPC). Bulletin of Engineering Geology and the Environment 2003;62:167-184 & erratum: pp. 185-185.

[28] Yang XL, Li L, Yin JH, Stability analysis of rock slopes with a modified Hoek–Brown failure criterion. International Journal for Numerical and Analytical Methods in Geomechanics 2004;28:181-190.

[29] Yang XL, Li L, Yin JH, Seismic and static stability analysis for rock slopes by a kinematical approach. Geotechnique 2004;54(8):543-549.

[30] Yang XL, Zou JF, Stability factors for rock slopes subjected to pore water pressure based on the Hoek-Brown failure criterion. International Journal of Rock Mechanics & Mining Science 2006;43:1146-1152.

[31] Zanbak C, Design Charts for rock slopes susceptible to toppling. Journal of Geotechnical Engineering, ASCE 1983;190(8):1039-1062.

[32] Siad L, Seismic stability analysis of fractured rock slopes by yield design theory. Soils dynamics and earthquake engineering 2003;23:203-212.

[33] Marinos V, Marinos P, Hoek E, The geological strength index: applications and limitations. Bulletin of Engineering Geology and the Environment 2005;64:55-65.

[34] Hoek E, Strength of jointed rock masses. Geotechnique 1983;33(3):187-223.

[35] Bieniaski ZT. Rock mass classification in rock engineering. In Exploration for rock engineering, proceedings of the symposium. 1976, Cape Town: Balkema.

[36] Barton N, Some new Q-value correlations to assist in site characterisation and tunnel design. International Journal of Rock Mechanics & Mining Sciences 2002;39(2):185-216.

[37] Hoek E, Rock Engineering. 2000 (http://www.rocscience.com/hoek/references/Published-Papers.htm).

[38] Hoek E, Brown ET, Practical estimates of rock mass strength. International Journal of Rock Mechanics & Mining Sciences 1997;34(8):1165-1186.

[39] Rocscience, 2D limit equilibrium analysis software, Slide 5.0. (www.rocscience.com).

[40] Bishop AW, The use of slip circle in stability analysis of slopes. Geotechnique 1955;5(1):7-17.

Table 1.
Comparisons of safety factors between the Hoek-Brown strength parameters and the equivalent Mohr-Coulomb parameters

			LIMIT ANALYSIS - LOWER BOUND		SLIDE - Limit Equilibrium using equivalent Mohr-Coulomb Parameters							
			Nonlinear Hoek-Brown		Nonlinear Hoek-Brown		Eq. (7), (8) & (9) Linear Mohr-Coulomb		Eq. (7), (8) & (12) Linear Mohr-Coulomb		Eq. (7), (8) & (13) Linear Mohr-Coulomb	
β	*GSI*	m_i	$(\sigma_{ci}/\gamma H)_{crit}$	*F*	*F1*	*%Diff*	*F2*	*%Diff*	*F3*	*%Diff*	*F4*	*%Diff*
75	100	5	0.360	1	0.963	-3.7%	1.008	1%	1.028	3%	-	-
75	100	15	0.278	1	0.999	-0.1%	1.164	16%	1.042	4%	-	-
75	100	25	0.228	1	1.002	0.2%	1.218	22%	1.079	8%	-	-
75	100	35	0.194	1	1.004	0.4%	1.286	29%	1.112	11%	-	-
75	70	5	1.703	1	0.988	-1.2%	1.081	8%	1.025	2%	-	-
75	70	15	1.169	1	1.002	0.2%	1.287	29%	1.081	8%	-	-
75	70	25	0.890	1	1.005	0.5%	1.35	35%	1.124	12%	-	-
75	70	35	0.717	1	1.016	1.6%	1.394	39%	1.156	16%	-	-
75	50	5	4.980	1	0.997	-0.3%	1.154	15%	1.036	4%	-	-
75	50	15	2.988	1	1.004	0.4%	1.336	34%	1.119	12%	-	-
75	50	25	2.156	1	1.018	1.8%	1.425	43%	1.148	15%	-	-
75	50	35	1.668	1	1.024	2.4%	1.45	45%	1.174	17%	-	-
75	30	5	15.011	1	1.001	0.1%	1.248	25%	1.047	5%	-	-
75	30	15	8.576	1	1.016	1.6%	1.459	46%	1.136	14%	-	-
75	30	25	5.824	1	1.025	2.5%	1.51	51%	1.173	17%	-	-
75	30	35	4.327	1	1.033	3.3%	1.516	52%	1.194	19%	-	-
75	10	5	93.721	1	1.004	0.4%	1.224	22%	1.018	2%	-	-
75	10	15	53.362	1	1.023	2.3%	1.504	50%	1.126	13%	-	-
75	10	25	35.186	1	1.035	3.5%	1.605	61%	1.185	19%	-	-
75	10	35	24.994	1	1.046	4.6%	1.642	64%	1.21	21%	-	-
60	100	5	0.232	1	1.001	0.1%	1.033	3%	1.043	4%	-	-

Table 1. (continued)

			LIMIT ANALYSIS - LOWER BOUND		SLIDE - Limit Equilibrium using equivalent Mohr-Coulomb Parameters							
			Nonlinear Hoek-Brown		Nonlinear Hoek-Brown		Eq. (7), (8) & (9) Linear Mohr-Coulomb		Eq. (7), (8) & (12) Linear Mohr-Coulomb		Eq. (7), (8) & (13) Linear Mohr-Coulomb	
β	*GSI*	m_i	$(\sigma_{ci}/\gamma H)_{crit}$	*F*	*F1*	*%Diff*	*F2*	*%Diff*	*F3*	*%Diff*	*F4*	*%Diff*
60	100	15	0.130	1	1.004	0.4%	1.114	11%	1.026	3%	-	-
60	100	25	0.088	1	1.004	0.4%	1.146	15%	1.035	3%	-	-
60	100	35	0.066	1	1.004	0.4%	1.141	14%	1.04	4%	-	-
60	70	5	0.946	1	1.013	1.3%	1.059	6%	1.024	2%	-	-
60	70	15	0.435	1	1.004	0.4%	1.143	14%	1.033	3%	-	-
60	70	25	0.276	1	1.004	0.4%	1.161	16%	1.043	4%	-	-
60	70	35	0.200	1	1.005	0.5%	1.183	18%	1.047	5%	-	-
60	50	5	2.337	1	1.005	0.5%	1.124	12%	1.026	3%	-	-
60	50	15	0.953	1	1.004	0.4%	1.171	17%	1.036	4%	-	-
60	50	25	0.584	1	1.008	0.8%	1.176	18%	1.046	5%	-	-
60	50	35	0.419	1	1.009	0.9%	1.172	17%	1.049	5%	-	-
60	30	5	6.439	1	1.009	0.9%	1.15	15%	1.023	2%	-	-
60	30	15	2.317	1	1.009	0.9%	1.197	20%	1.044	4%	-	-
60	30	25	1.356	1	1.01	1.0%	1.201	20%	1.049	5%	-	-
60	30	35	0.945	1	1.011	1.1%	1.23	23%	1.051	5%	-	-
60	10	5	38.926	1	1.004	0.4%	1.183	18%	1.013	1%	-	-
60	10	15	11.734	1	1.013	1.3%	1.257	26%	1.048	5%	-	-
60	10	25	5.928	1	1.017	1.7%	1.261	26%	1.054	5%	-	-
60	10	35	3.729	1	1.018	1.8%	1.258	26%	1.059	6%	-	-
45	100	5	0.135	1	1	0.0%	1.008	1%	1.022	2%	1.027	3%
45	100	15	0.058	1	1.005	0.5%	1.041	4%	1.003	0%	1.086	9%
45	100	25	0.036	1	1.012	1.2%	1.047	5%	1.003	0%	1.11	11%

Table 1. (continued)

			LIMIT ANALYSIS - LOWER BOUND		SLIDE - Limit Equilibrium using equivalent Mohr-Coulomb Parameters							
			Nonlinear Hoek-Brown		Nonlinear Hoek-Brown		Eq. (7), (8) & (9) Linear Mohr-Coulomb		Eq. (7), (8) & (12) Linear Mohr-Coulomb		Eq. (7), (8) & (13) Linear Mohr-Coulomb	
β	GSI	m_i	$(\sigma_{ci}/\gamma H)_{crit}$	F	$F1$	$\%Diff$	$F2$	$\%Diff$	$F3$	$\%Diff$	$F4$	$\%Diff$
45	100	35	0.026	1	1.015	1.5%	1.06	6%	1.005	0%	1.126	13%
45	70	5	0.469	1	1.001	0.1%	1.038	4%	1.001	0%	1.055	5%
45	70	15	0.176	1	1.012	1.2%	1.08	8%	1.002	0%	1.098	10%
45	70	25	0.108	1	1.017	1.7%	1.06	6%	1.007	1%	1.113	11%
45	70	35	0.077	1	1.019	1.9%	1.061	6%	1.009	1%	1.123	12%
45	50	5	1.046	1	1.004	0.4%	1.045	4%	1.001	0%	1.063	6%
45	50	15	0.369	1	1.009	0.9%	1.065	6%	1.004	0%	1.098	10%
45	50	25	0.222	1	1.02	2.0%	1.066	7%	1.01	1%	1.11	11%
45	50	35	0.158	1	1.021	2.1%	1.044	4%	1.011	1%	1.118	12%
45	30	5	2.593	1	1.011	1.1%	1.066	7%	0.999	0%	1.06	6%
45	30	15	0.829	1	1.018	1.8%	1.07	7%	1.007	1%	1.094	9%
45	30	25	0.480	1	1.021	2.1%	1.076	8%	1.01	1%	1.11	11%
45	30	35	0.334	1	1.024	2.4%	1.085	9%	1.011	1%	1.118	12%
45	10	5	13.585	1	1.014	1.4%	1.087	9%	1	0%	1.039	4%
45	10	15	3.155	1	1.023	2.3%	1.106	11%	1.005	0%	1.08	8%
45	10	25	1.552	1	1.023	2.3%	1.107	11%	1.009	1%	1.103	10%
45	10	35	0.969	1	1.026	2.6%	1.079	8%	1.01	1%	1.115	12%
30	100	5	0.070	1	1.014	1.4%	0.988	-1%	-	-	1	0%
30	100	15	0.026	1	1.02	2.0%	0.999	0%	-	-	1.024	2%
30	100	25	0.016	1	1.023	2.3%	1.003	0%	-	-	1.036	4%
30	100	35	0.011	1	1.024	2.4%	1.007	1%	-	-	1.044	4%
30	70	5	0.218	1	1.018	1.8%	0.985	-2%	-	-	1.011	1%

Table 1. (continued)

			LIMIT ANALYSIS - LOWER BOUND		SLIDE - Limit Equilibrium using equivalent Mohr-Coulomb Parameters							
			Nonlinear Hoek-Brown		Nonlinear Hoek-Brown		Eq. (7), (8) & (9) Linear Mohr-Coulomb		Eq. (7), (8) & (12) Linear Mohr-Coulomb		Eq. (7), (8) & (13) Linear Mohr-Coulomb	
β	*GSI*	m_i	$(\sigma_{ci}/\gamma H)_{crit}$	*F*	*F1*	*%Diff*	*F2*	*%Diff*	*F3*	*%Diff*	*F4*	*%Diff*
30	70	15	0.075	1	1.023	2.3%	0.996	0%	-	-	1.028	3%
30	70	25	0.045	1	1.024	2.4%	1.004	0%	-	-	1.035	3%
30	70	35	0.032	1	1.025	2.5%	1.01	1%	-	-	1.04	4%
30	50	5	0.461	1	1.02	2.0%	0.993	-1%	-	-	1.014	1%
30	50	15	0.153	1	1.024	2.4%	1.003	0%	-	-	1.026	3%
30	50	25	0.091	1	1.025	2.5%	1.024	2%	-	-	1.032	3%
30	50	35	0.065	1	1.026	2.6%	1.008	1%	-	-	1.036	4%
30	30	5	1.057	1	1.022	2.2%	1.001	0%	-	-	1.012	1%
30	30	15	0.323	1	1.026	2.6%	1.003	0%	-	-	1.026	3%
30	30	25	0.185	1	1.026	2.6%	1.005	0%	-	-	1.031	3%
30	30	35	0.129	1	1.027	2.7%	1.004	0%	-	-	1.035	3%
30	10	5	4.363	1	1.023	2.3%	1.002	0%	-	-	1.006	1%
30	10	15	0.943	1	1.025	2.5%	1.007	1%	-	-	1.023	2%
30	10	25	0.460	1	1.026	2.6%	0.996	0%	-	-	1.033	3%
30	10	35	0.286	1	1.026	2.6%	1.004	0%	-	-	1.04	4%
10	100	5	0.026	1	1.009	0.9%	1.067	7%	-	-	1	0%
10	100	15	0.009	1	1.011	1.1%	1.079	8%	-	-	0.987	-1%
10	100	25	0.005	1	1.011	1.1%	1.091	9%	-	-	0.985	-2%
10	100	35	0.004	1	1.012	1.2%	1.094	9%	-	-	0.986	-1%
10	70	5	0.078	1	1.01	1.0%	1.069	7%	-	-	0.994	-1%
10	70	15	0.026	1	1.01	1.0%	1.087	9%	-	-	0.987	-1%
10	70	25	0.015	1	1.011	1.1%	1.091	9%	-	-	0.985	-2%

Table 1. (continued)

			LIMIT ANALYSIS - LOWER BOUND		SLIDE - Limit Equilibrium using equivalent Mohr-Coulomb Parameters							
			Nonlinear Hoek-Brown		Nonlinear Hoek-Brown		Eq. (7), (8) & (9) Linear Mohr-Coulomb		Eq. (7), (8) & (12) Linear Mohr-Coulomb		Eq. (7), (8) & (13) Linear Mohr-Coulomb	
β	*GSI*	m_i	$(\sigma_{ci}/\gamma H)_{cri}$	*F*	*F1*	*%Diff*	*F2*	*%Diff*	*F3*	*%Diff*	*F4*	*%Diff*
10	70	35	0.011	1	1.011	1.1%	1.094	9%	-	-	0.985	-2%
10	50	5	0.158	1	1.01	1.0%	1.067	7%	-	-	0.996	0%
10	50	15	0.052	1	1.01	1.0%	1.055	5%	-	-	0.989	-1%
10	50	25	0.031	1	1.011	1.1%	1.081	8%	-	-	0.986	-1%
10	50	35	0.022	1	1.011	1.1%	1.084	8%	-	-	0.985	-2%
10	30	5	0.334	1	1.01	1.0%	1.05	5%	-	-	0.997	0%
10	30	15	0.101	1	1.011	1.1%	1.068	7%	-	-	0.99	-1%
10	30	25	0.058	1	1.011	1.1%	1.072	7%	-	-	0.988	-1%
10	30	35	0.040	1	1.011	1.1%	1.075	8%	-	-	0.986	-1%
10	10	5	0.994	1	1.012	1.2%	1.036	4%	-	-	0.994	-1%
10	10	15	0.211	1	1.013	1.3%	1.039	4%	-	-	0.985	-2%
10	10	25	0.103	1	1.013	1.3%	1.041	4%	-	-	0.985	-2%
10	10	35	0.064	1	1.013	1.3%	1.032	3%	-	-	0.986	-1%

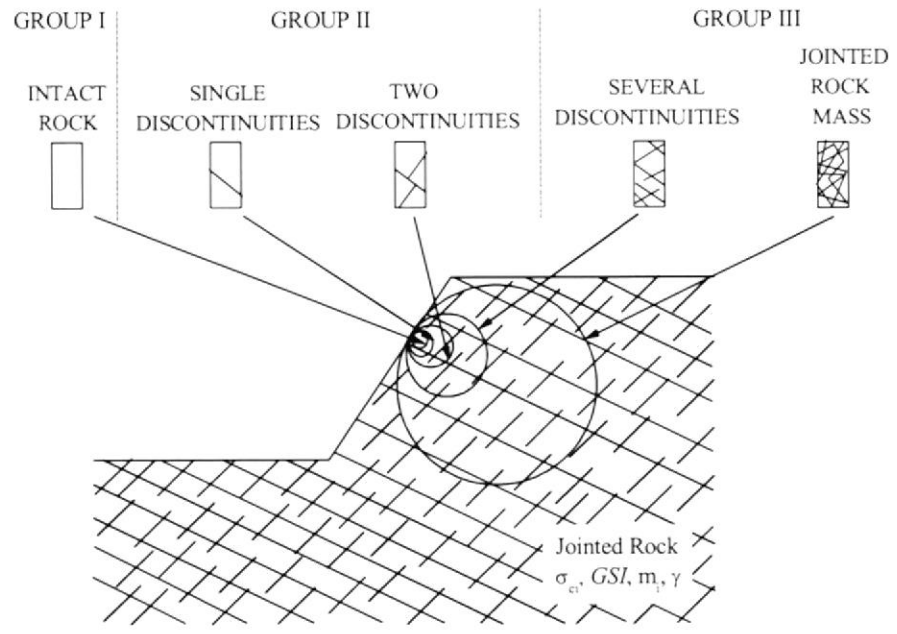

Fig. 1. Applicability of the Hoek-Brown failure criterion for slope stability problems.

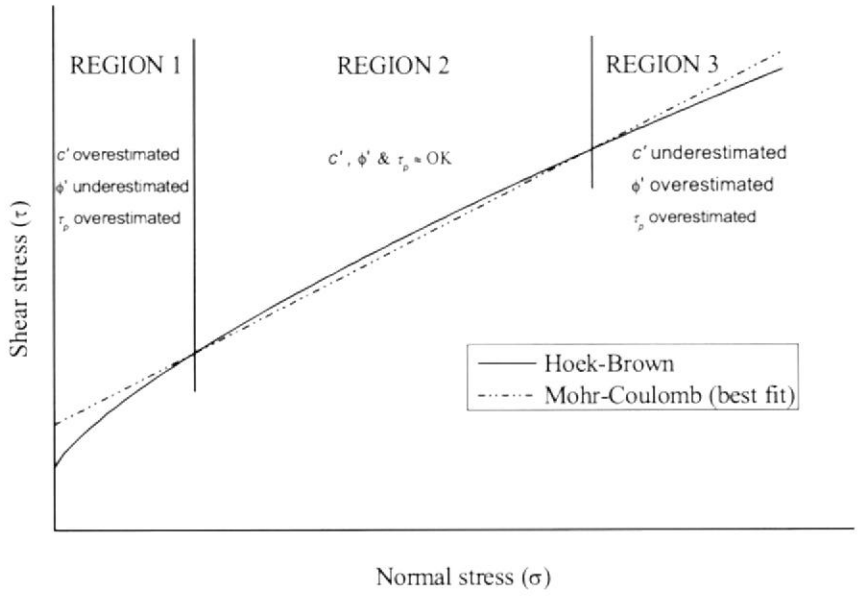

Fig. 2. Hoek-Brown and equivalent Mohr-Coulomb criteria.

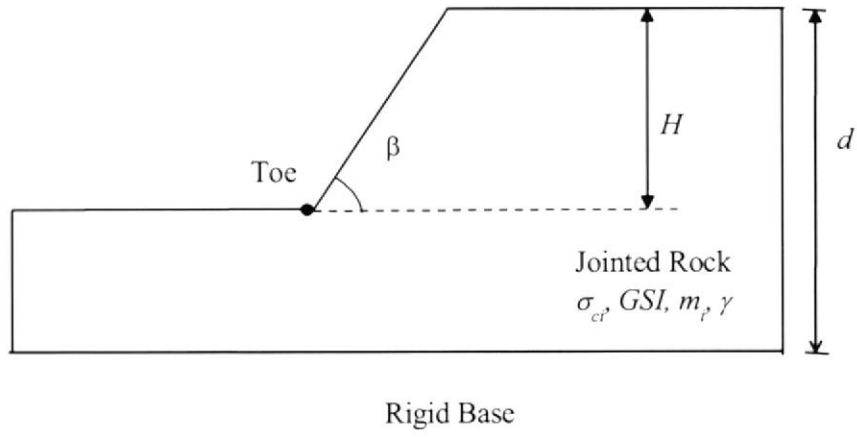

Fig. 3. Problem definition.

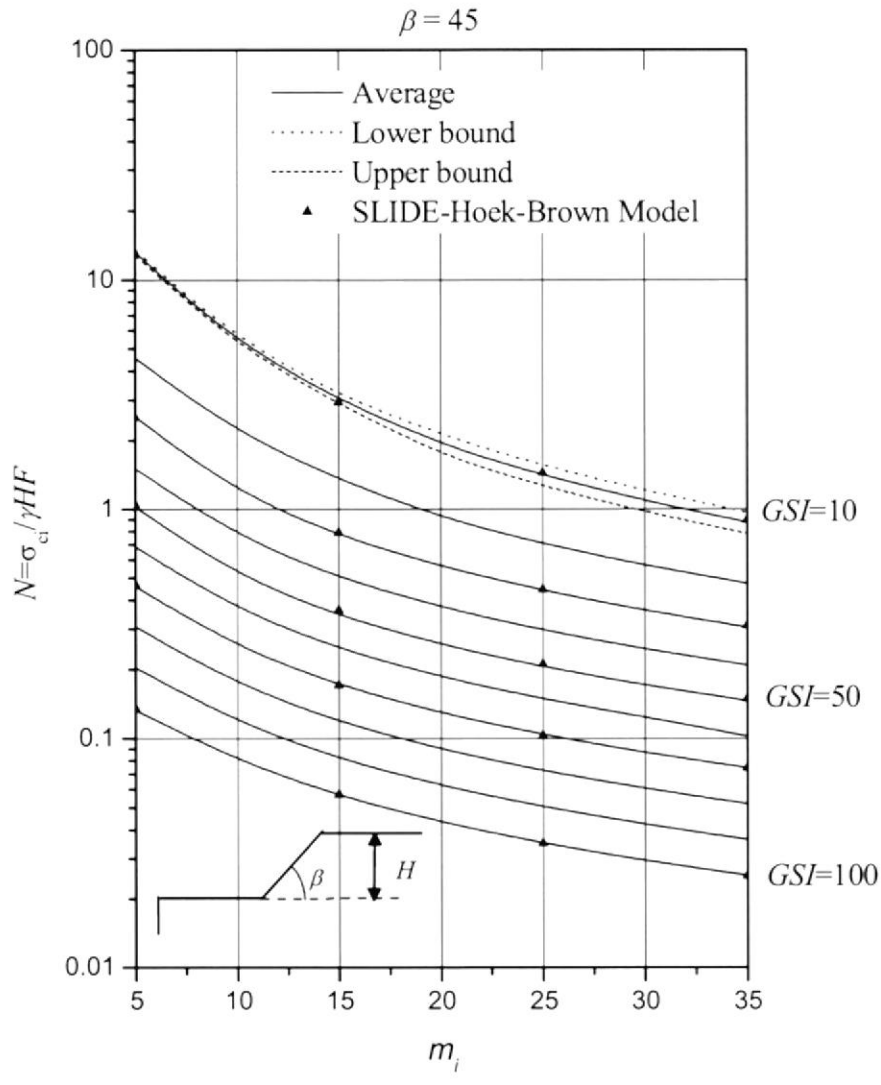

Fig. 4. Average finite element limit analysis solutions of stability numbers ($\beta = 45^{\circ}$).

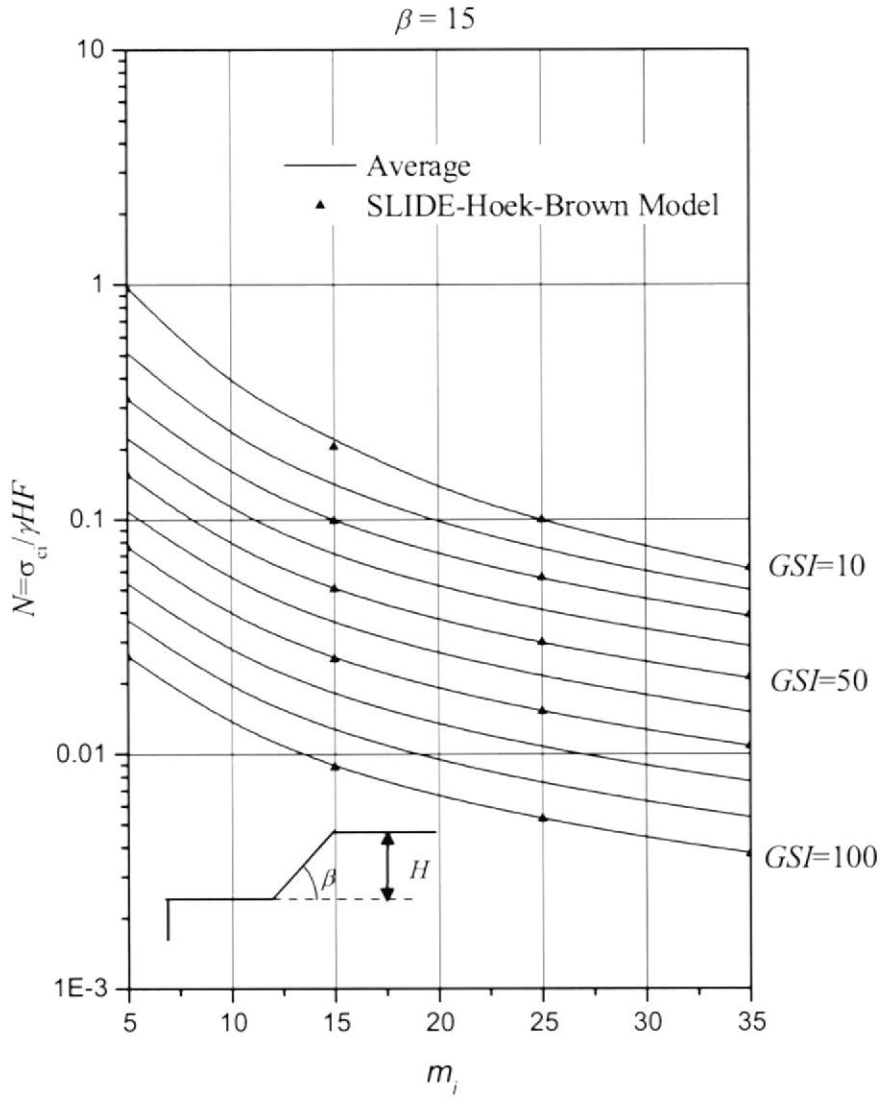

Fig. 5. Average finite element limit analysis solutions of stability numbers ($\beta = 15^{\circ}$).

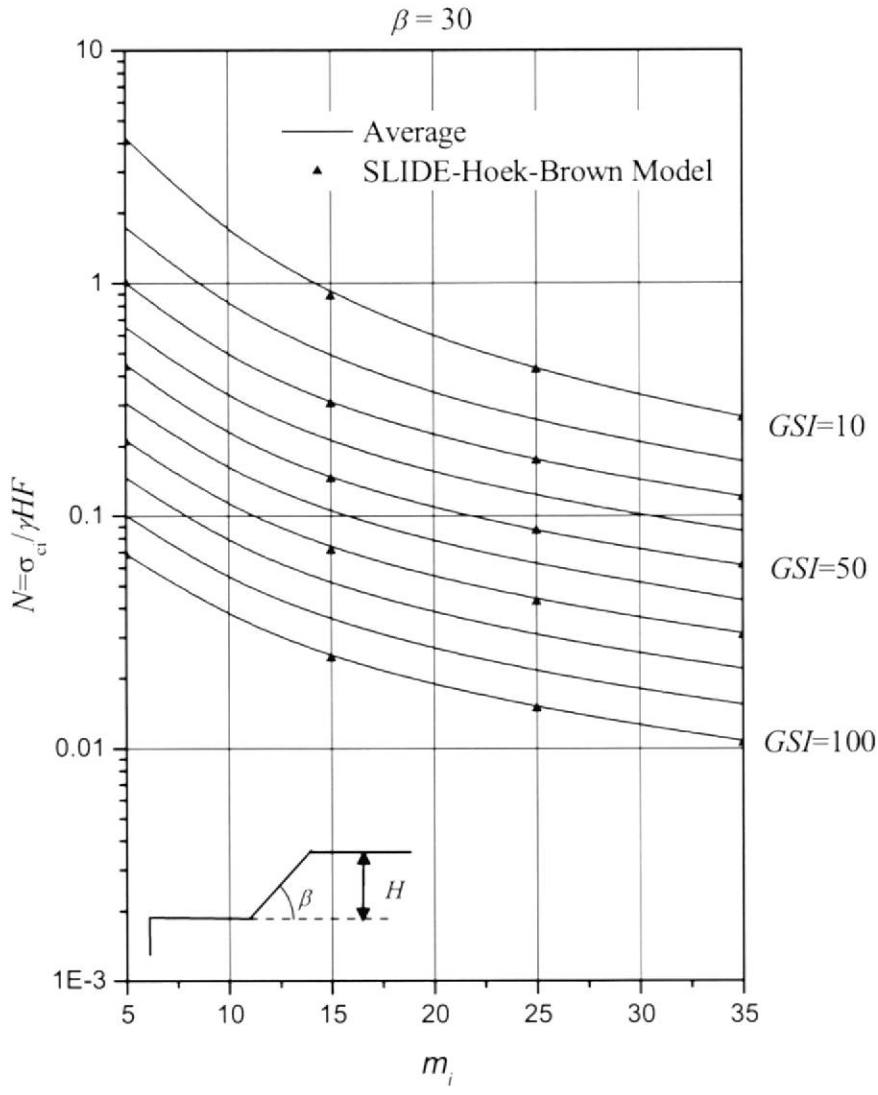

Fig. 6. Average finite element limit analysis solutions of stability numbers ($\beta = 30^{\circ}$).

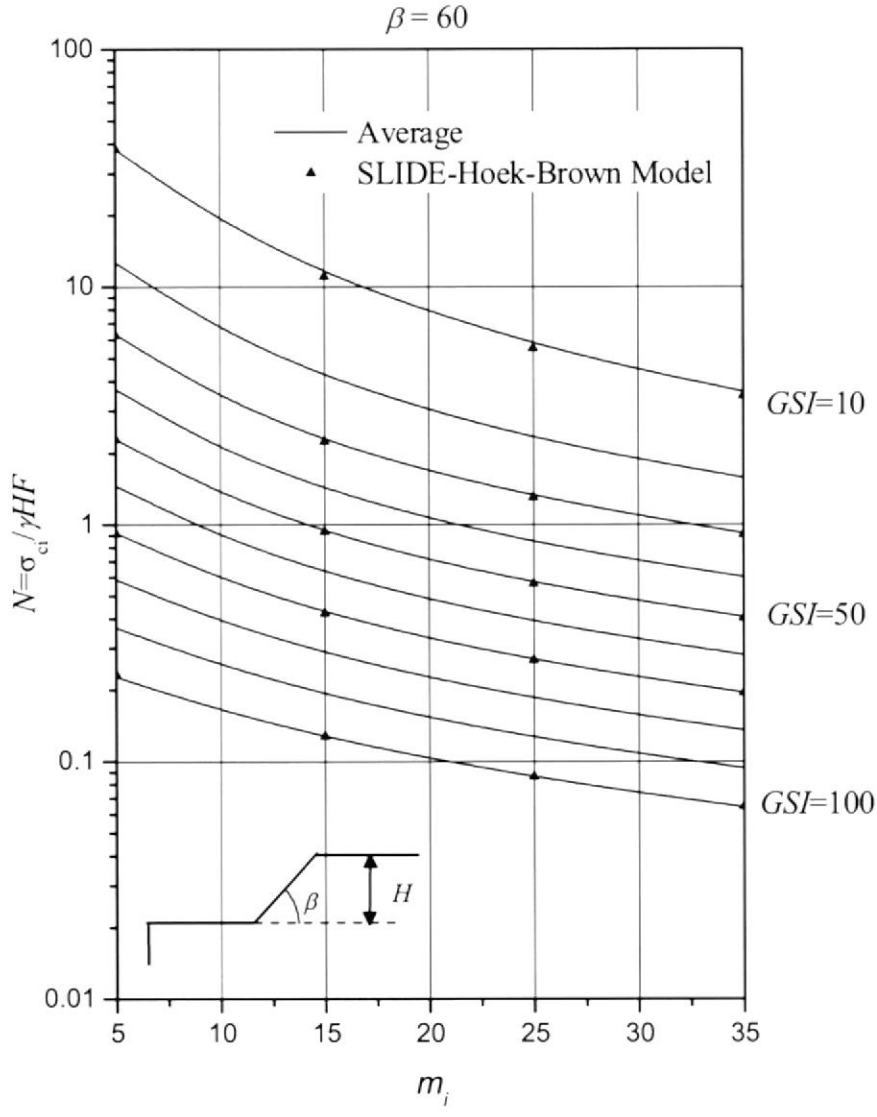

Fig. 7. Average finite element limit analysis solutions of stability numbers ($\beta = 60^{\circ}$).

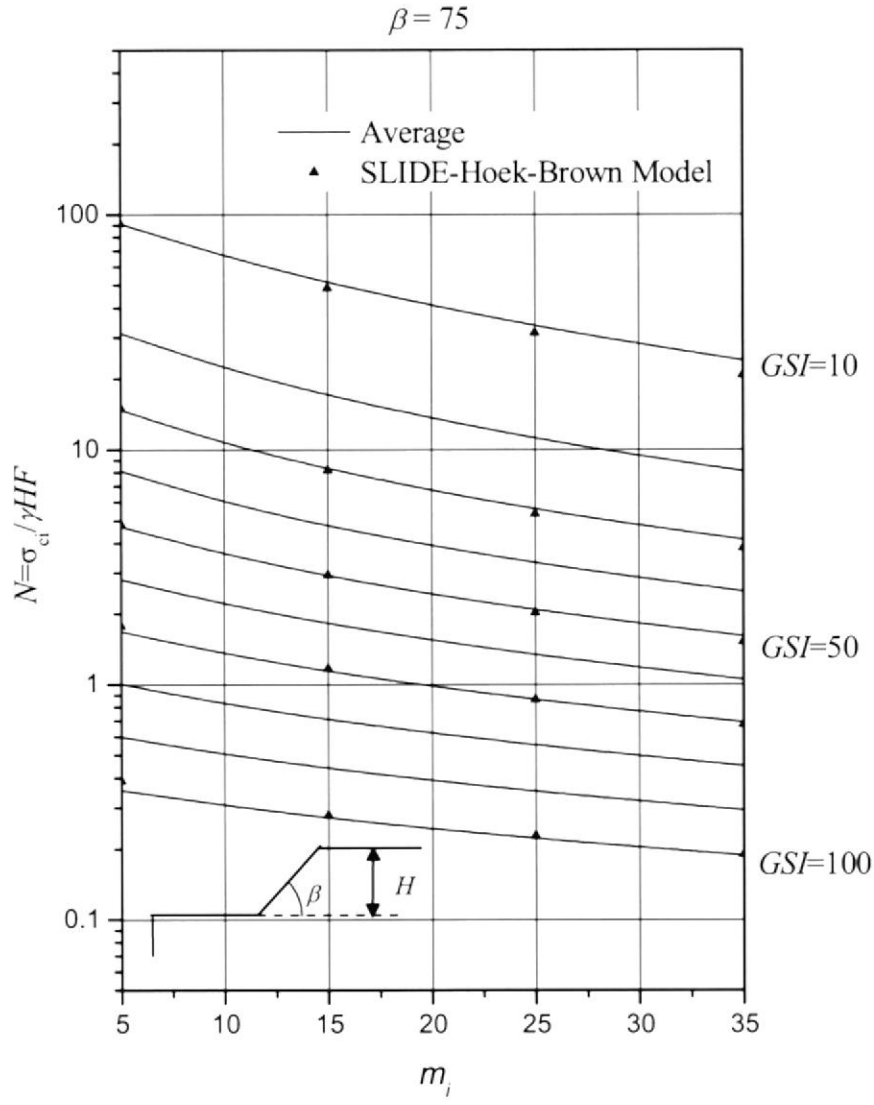

Fig. 8. Average finite element limit analysis solutions of stability numbers ($\beta = 75^{\circ}$).

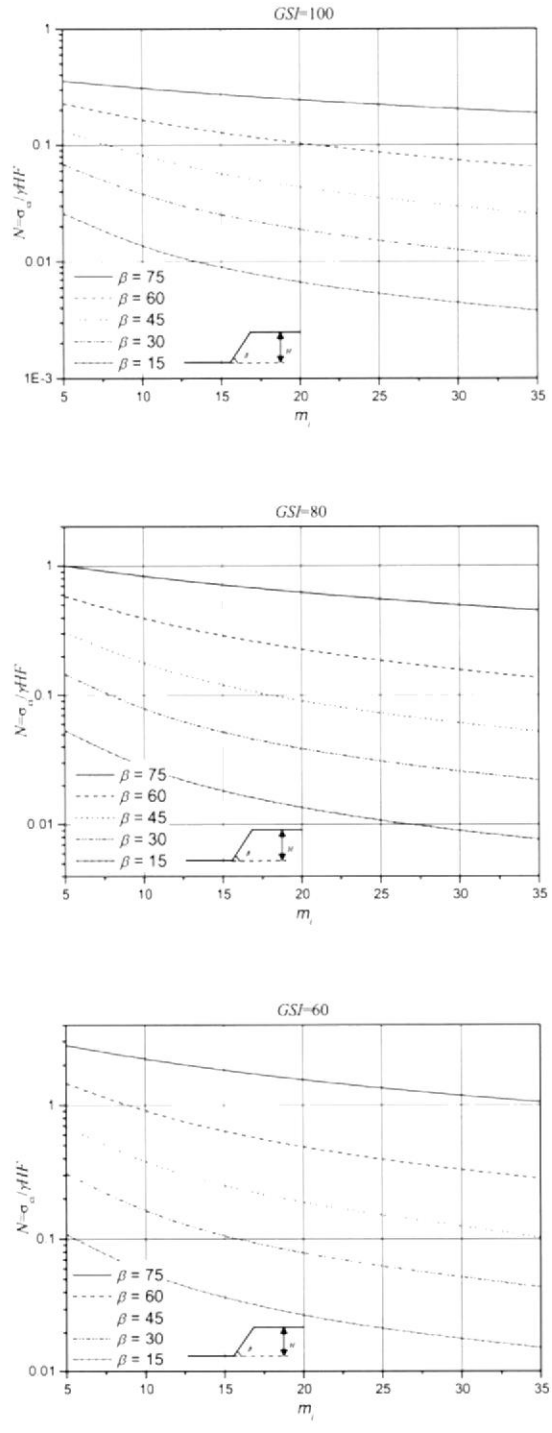

Fig. 9. Average finite element limit analysis solutions of stability numbers (GSI = 100, 80 and 60).

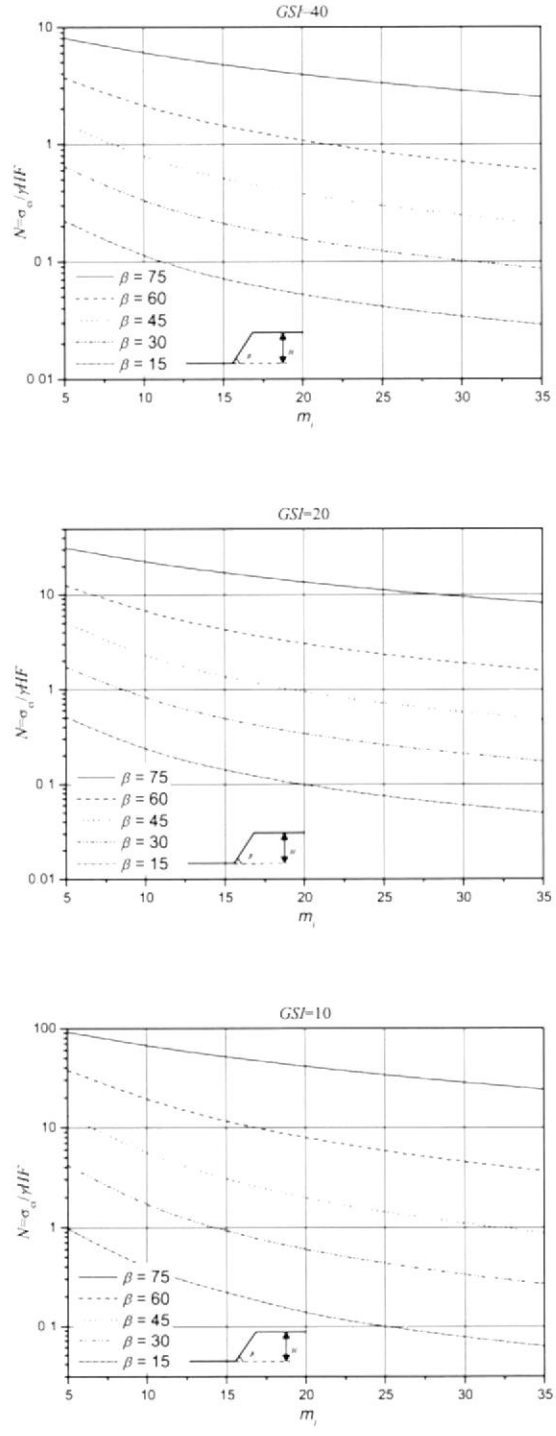

Fig. 10. Average finite element limit analysis solutions of stability numbers (GSI = 40, 20 and 10).

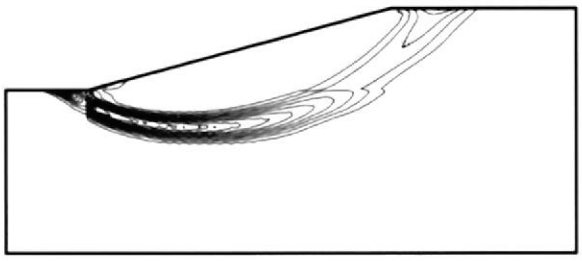

$\beta = 15^{\circ}$

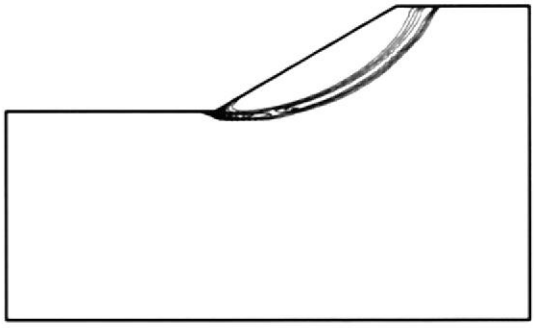

$\beta = 30^{\circ}$

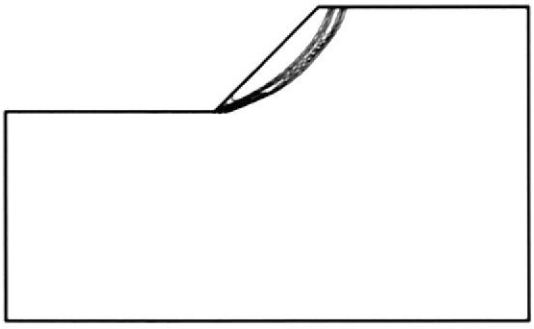

$\beta = 45^{\circ}$

Fig. 11. Upper bound plastic zones with the different slope angles ($GSI = 70$ and $m_i = 15$).

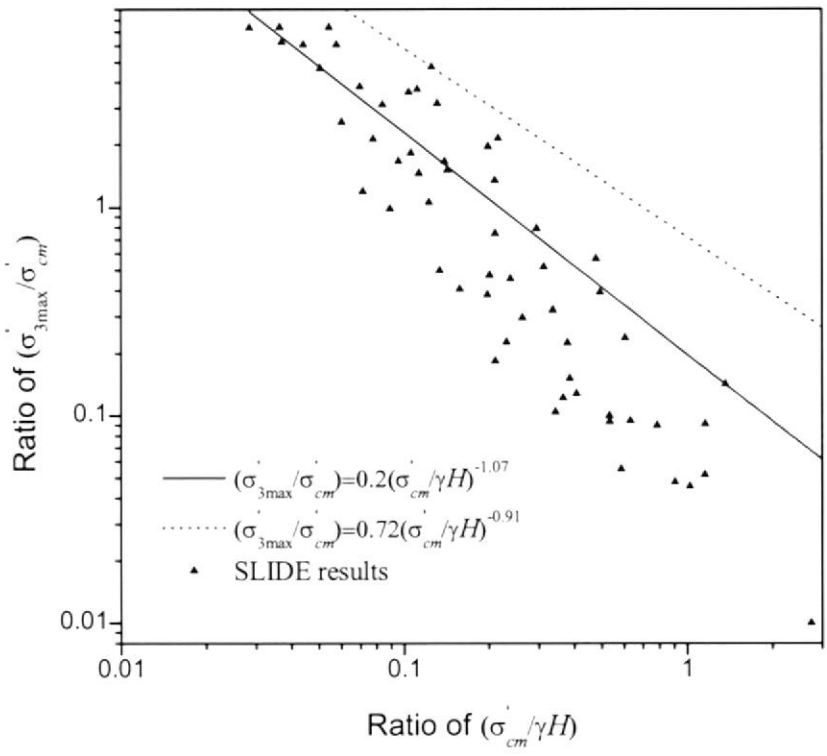

Fig. 12. Relationship for the calculation of $\sigma'_{3\max}$ between equivalent Mohr-Coulomb and Hoek-Brown parameters for steep slopes ($\beta \geq 45^{\circ}$).

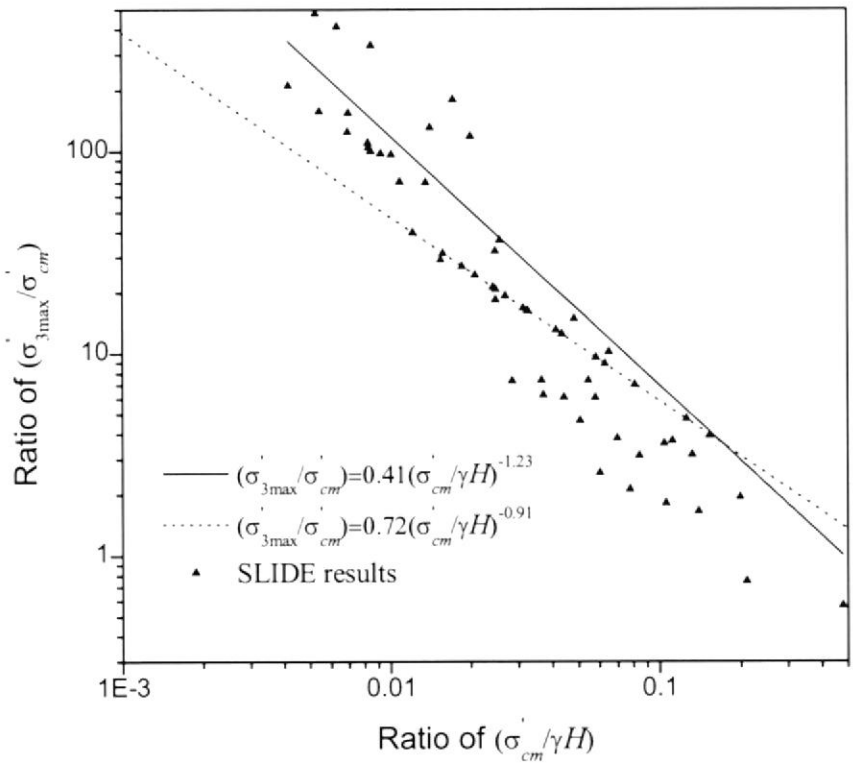

Fig. 13. Relationship for the calculation of σ'_{3max} between equivalent Mohr-Coulomb and Hoek-Brown parameters for gentle slopes ($\beta < 45^{\circ}$).

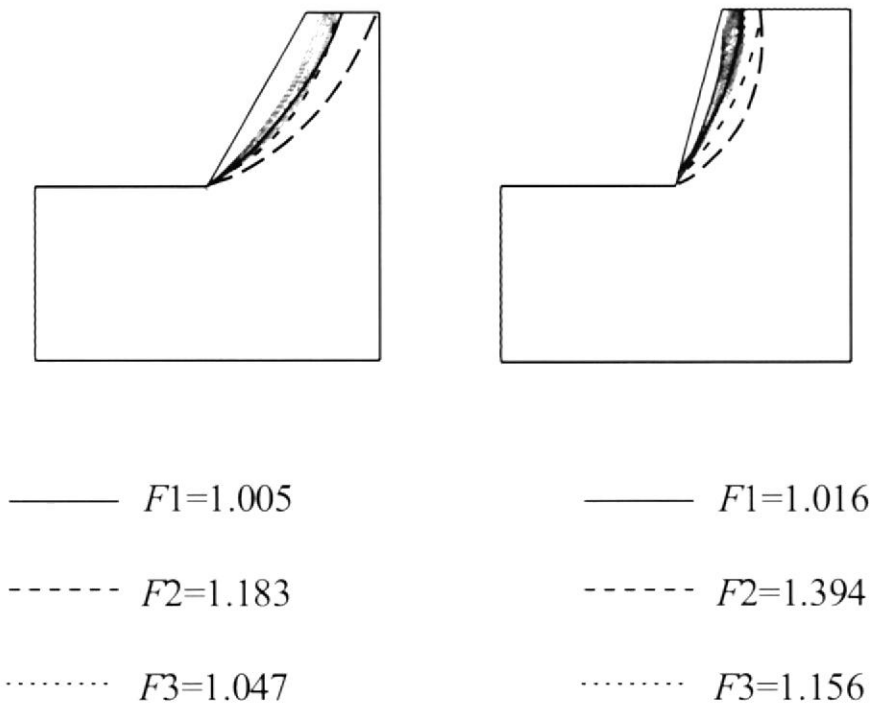

Fig. 14. Comparison between upper bound plastic zones and failure surfaces from different strength parameters ($GSI = 70$ and $m_i = 35$).

BIBLIOGRAFÍA

GAVILANEZ H., ANDRADE B., *Introducción a la Ingeniería de Túneles: caracterización, clasificación y análisis geomecánico de macizos rocosos*. A.I.M.E del Ecuador, 2004. Capítulo 3 y Apéndice 5

CARRILO M., LINKIMER L., RODRÍGUEZ A., ZÚÑIGA H., *Clasificación Geomecánica y Análisis de Estabilidad de Taludes del Macizo Rocoso Coris, Cartago, Costa Rica,* publicado en la Revista Geológica de América Central, 2002.

HERRERA F., *Análisis de Estabilidad de Taludes*, Editorial GEOTECNIA 2000, Madrid – España, Páginas. 5 – 32.

LI J., MERIFIELD R., LYAMIN A., *Stability Charts for Rock Slopes Based on the Hoek – Brown Failure Criterion*, Publicación de la Universidad de Western Australia, sin fecha exacta de publicación.